

# **Anticipatory Fleet Repositioning for Shared-use Autonomous Mobility Services: An Optimization and Learning-Based Approach**

**Monika Filipovska**, Corresponding Author

University of Connecticut, Department of Civil and Environmental Engineering

email: [monika.filipovska@uconn.edu](mailto:monika.filipovska@uconn.edu)

ORCID: 0000-0002-2718-4722

**Michael Hyland**

University of California-Irvine, Department of Civil and Environmental Engineering,

University of California-Irvine, Institute of Transportation Studies,

email: [hylandm@uci.edu](mailto:hylandm@uci.edu)

ORCID: 0000-0001-8394-8064

**Haimanti Bala**

University of Connecticut, Department of Civil and Environmental Engineering,

email: [haimanti.bala@uconn.edu](mailto:haimanti.bala@uconn.edu)

ORCID: 0000-0001-7241-522X

Declarations of interest: none

## Abstract

With the development of mobility-on-demand services, increasing sources of rich transportation data, and the advent of autonomous vehicles (AVs), there are significant opportunities for shared-use AV mobility services (SAMSs) to provide accessible and demand-responsive personal mobility. The operation of SAMS vehicle fleets involves multiple interrelated decisions and goals, primarily focusing on demand-responsive passenger-vehicle matching with the goal of system-wise efficiency and service quality. This paper focuses on the problem of anticipatory repositioning of idle vehicles in a SAMS fleet to enable better assignment decisions in serving future demand. The rebalancing problem is formulated as a Markov Decision Process and a reinforcement learning-based approach using an advantage actor critic (A2C) method is proposed to learn a rebalancing policy that anticipates future demand and cooperates with an optimization-based assignment strategy. The proposed formulation and solution approach allow for centralized repositioning decisions for the entire vehicle fleet, but ensure that the problem size does not change with the size of the vehicle fleet.

Using an agent-based simulation tool and New York City taxi data to simulate demand for rides in the SAMS system, two versions of the A2C AV repositioning approach are tested. The first version, A2C-AVR(A), observes past demand for rides and learns to anticipate future demand. The second version, A2C-AVR(B), receives demand forecasts. The models are compared to one another and an alternative optimization-based rebalancing approach from the literature that uses the same demand forecasts as model (B). Numerical experiments demonstrate that the A2C-AVR approaches significantly reduce mean passenger waiting times relative to the optimization-based approach, at the expense of slightly increased percentage of empty fleet miles travelled. The experiments show that the A2C-AVR(A) approach performs comparably to approach (B), indicating its ability to anticipate future demand simply based on past demand observations. Testing with various demand and time-of-day scenarios, and an alternative assignment strategy, the experiments demonstrate the models' transferability to cases unseen at the training stage.

**Keywords:** Autonomous Vehicles, Ridesourcing, Fleet Management, Mobility-as-a-Service, Demand Responsive Transportation

# 1 Introduction

## 1.1 Motivation and Background

The rapid development of mobility-on-demand (MOD) services in recent years along with the emergence of wireless communication technologies and rich data sources are redefining personal mobility. MOD is envisioned to help promote demand-responsive and accessible multimodal transportation, ultimately improving transportation efficiency and equity. Ridesourcing services in the MOD space, such as Uber, Lyft, Didi, etc. have created a new set of opportunities and challenges for advancing mobility. By providing unprecedented transportation alternatives and access to personalized mobility, they are creating significant economic and social value (Federal Transit Administration, 2021). However, by providing rides for previously under-served demand for travel they also increase vehicle-based congestion. With the advent of autonomous vehicles (AVs), and their expected inclusion in mobility service fleets, significant research related to the operation and management of shared-use AV mobility services (SAMSs) has emerged over the past decade.

The transportation literature focuses on two primary problem classes in this domain, which have largely been treated independently: (a) forecasting demand and user requests, and (b) developing operational strategies for the efficient operations of SAMS fleets with known or predicted demand. Demand forecasting focuses on producing useful models of the ride demand patterns in order to accurately predict future demand in a SAMS system (Sayarshad and Chow, 2016). Operational strategies for SAMS fleets focus on two types of problems: the assignment of AVs in the fleet to incoming demand or ride requests (Hyland and Mahmassani, 2018, 2017; Maciejewski et al., 2016), and the management of unutilized vehicles in the fleet towards improving the systems operational efficiency (Dandl and Bogenberger, 2019; Fagnant and Kockelman, 2014; Sayarshad and Chow, 2017). While specific problem formulations can differ, the management of unutilized fleet vehicles typically involves the repositioning of idle AVs in anticipation of future demand. The forecasting and operational problems are certainly not independent of one another, and in practice, mobility service providers need to consider these problems jointly. Operational solutions are heavily dependent on the quality of the forecasts, and the forecasts are only as useful as they can contribute to the efficiency objectives of the operational problems. This relationship between the forecasting and operational problems has been demonstrated in recent studies (Dandl et al., 2019; Hyland et al., 2019). Furthermore, the two types of operational problems, i.e., the passenger assignment and fleet repositioning, are also highly interrelated with one another. Assignment decisions determine the distribution of idle vehicles available for repositioning, while the repositioning decisions enable future assignment during repositioning or after it is completed. Nevertheless, the relationship between the two types of operational decisions is not straightforward and can be difficult to capture or model via explicit constraints. Motivated by the need for integration of the forecasting and operational SAMS problem, this study presents a cohesive SAMS operational framework focused on an anticipatory learning-based fleet repositioning approach integrated with an optimization-based assignment approach.

## 1.2 Problem Statement and Contribution

This paper focuses on developing an approach for anticipatory repositioning of idle AVs that cooperates with an AV-to-passenger assignment strategy in order to improve the overall system

efficiency and quality of service. The implementation of the approach for fleet repositioning requires the anticipation of future demand and adaptation to passenger assignment decisions (both past and future) that utilize the idle and repositioning vehicles of the fleet. Therefore, the problem formulation requires integrating all three components of the SAMS system: the unknown demand-generating process, the assignment of AVs to passenger requests, and the management of idle AVs. The current study formulates the vehicle repositioning problem as a Markov Decision Process (MDP) that interacts with the incoming demand and assignment decision-making to find a solution that accounts for the system’s evolution as a result of both. We present a reinforcement learning (RL) approach to devise an idle-vehicle repositioning policy for a given assignment policy and unknown demand-generating process. The learning-based approach can observe predictions of future demand or simply rely on past demand observations and implicitly learn the demand patterns.

This paper makes several contributions to the literature. Broadly, it demonstrates how the two problem classes can be brought together in a way that explicitly models the operational problem while implicitly learning to anticipate demand. Specifically, the paper (1) solves the AV fleet rebalancing problem via a single-agent RL approach for a centralized controller that operates the entire fleet, (2) bypasses the need for explicit demand forecasting via the RL operational strategy that implicitly anticipates future demand, (3) integrates the RL-based SAMS fleet repositioning strategy with an optimization-based fleet assignment approach, and (4) demonstrates the transferability of the proposed RL-based approach to unseen demand patterns and new assignment strategies not encountered in the model’s training stage.

The remainder of the paper is organized as follows. Section 2 presents a review of the relevant literature, followed by the notation and problem definition in Section 3. The solution approach is presented in Section 4, followed by numerical experiments in Section 5. Section 6 concludes the paper.

## 2 Literature Review

The literature on SAMS has grown significantly in the past decade, addressing problems in various contexts and problem settings. This review focuses on the studies most relevant to this paper, for a detailed review of SAMS, please refer to Narayanan et al. (2020) who present a comprehensive review of research on shared autonomous vehicles (SAV) services, including their foreseen impacts in terms of traffic and safety, travel behavior, transport supply, the economy, land use, environment and governance. It should be noted that various terms are often used interchangeably in the literature, including SAMS, SAV services, and autonomous mobility-on-demand (AMoD) systems.

Early literature on SAMS defines and classifies the associated AV fleet operational problems. Hyland and Mahmassani (2017) classify the problems as dynamic, multivehicle pickup and delivery problems (PDPs) with time-window constraints. The authors define the AV fleet management problem in terms of various components, including information availability (global and local) and processing (centralized and decentralized). They also introduce novel taxonomic categories, including whether or not vehicle repositioning is included, the type of underlying network used and how congestion is modeled in the system. These problem categories are useful in classifying existing problems in the literature and in defining new problem classes and solution algorithms.

The predominant class of SAMS problems are operational, including assignment or matching problems that determine the match between vehicles and passengers, and repositioning or

rebalancing problems that determine how idle vehicles are to be relocated within the service area in anticipation of future travel demand. Maciejewski et al. (2016) introduce and address the problem of passenger-vehicle assignment in a taxi dispatching system adapted for large-scale simulation. Hyland and Mahmassani (2018) present and compare optimization-based strategies for assigning AVs to immediate traveler demand requests in an on-demand SAMS with no shared rides. Hörl et al. (2021) present a comprehensive approach for the operation of a cost covering AMoD system with a predefined fleet size, where service costs, waiting times, and demand are in equilibrium. Extensions of these problems have also emerged. Accounting for shared rides, Alonso-Mora et al. (2017) approach the trip-vehicle assignment problem as a bipartite matching problem. Hyland and Mahmassani (2020) outline the operational benefits and challenges of accommodating shared rides in SAMSs. Dandl et al. (2021) consider the larger problem of a public-sector regulated mobility service provider (MSP) and present a tri-level model that includes the public-sector decision makers, the MSP, and the travelers.

A number of SAMS studies also introduce the vehicle repositioning problem. Two studies by Fagnant and Kockelman (2015, 2014) consider the additional vehicle miles travelled when SAMS vehicles are repositioned in anticipation of future demand. Another study (Pavone et al., 2012) considers vehicle rebalancing as a linear programming problem and develops a real-time rebalancing policy suited for highly variable environments. On the other hand, Sayarshad and Chow (2017) present a queueing-based formulation of the rebalancing problem along with a non-myopic solution using a Lagrangian decomposition heuristic. These studies primarily use a known random process that generates the demand as the basis for the relocation of idle vehicles in the fleet.

Demand forecasting for SAMS services is a less prominent class of problems in the literature. A few studies address the problem of developing demand forecasting methods that support the optimization problems for fleet operations, without defining the corresponding SAMS operational problems. A survey paper (Sayarshad and Chow, 2016) focusing on the demand forecasting methods for variations of the SAMS problem, categorize the existing approaches into offline and online methods, describing those methods relying on historical and real-time data access, respectively. Short-term demand forecasting studies have focused on predicting demand for carsharing (Müller and Bogenberger, 2015), taxi (Ihler et al., 2006; Moreira-Matias et al., 2013) and public transportation services (Zhong et al., 2016). Some studies also incorporate unconventional data into online demand-prediction models, such as social media data (Chaniotakis et al., 2016), or point-of-interest (POI) and meteorology data (Tong et al., 2017).

Though often approached as two separate problem classes in the literature, the operational (prescriptive analytics) problems and forecasting (predictive analytics) problems in the SAMS context are inherently interconnected. For one, mobility service providers in practice need to consider these problems jointly. Furthermore, the performance of the operational solutions is heavily dependent on the quality of the forecasting solutions. A few studies that have considered the joint problems and demonstrated their interconnectedness. Dandl et al. (2019) present results that indicate the inverse relationship between fleet performance and spatial aggregation of demand forecasts, despite the increasing forecast quality with spatial aggregation. The study also demonstrates that SAMS fleets benefit significantly from higher resolution demand forecasts.

Reinforcement learning (RL) methods have recently emerged as an alternative approach to formulating and solving SAMS problems, particularly using deep reinforcement learning (DRL). In this setting, learning-based approaches are employed to devise efficient algorithms, often without significantly compromising optimality. A recent survey of reinforcement learning for

ridesharing reviews the use of RL approaches for several problem types in the ridesharing system, including pricing, matching (i.e., passenger assignment), vehicle repositioning, routing, and shared rides, also referred to as ride-pooling (Qin et al., 2022). The forecasting and operational problem in RL frameworks can be integrated together so that assignment and/or rebalancing behaviors are learned explicitly along with an implicit learning of the underlying demand patterns. Thus, some RL formulations can bypass the need for an explicit demand forecast if RL agents are able to learn the demand patterns and make decisions in anticipation of future system states. Most commonly, studies employ multi-agent reinforcement learning (MARL) approaches, modeling a coordinated fleet of vehicles (Holler et al., 2019; Li et al., 2019; Oda and Joe-Wong, 2018; Singh et al., 2021). An alternative approach is presented by Gammelli et al. (2021), where a SAMS controller is modeled as a single agent making a multi-dimensional decision for the entire fleet. However, even here the underlying demand-generating random process is an input to the RL agent. This solution is also based on a prior study on learning how to operate a fleet of cars, again from the central controller’s perspective (Fluri et al., 2018). On the other hand, Gueriau and Dusparic (2018) present a decentralized RL-based approach for both rebalancing and assignment decisions with dynamic ridesharing, where each vehicle autonomously learns its behavior. In this case, no information about the demand patterns is given as an input, but rather the agents learn the demand patterns along with the desired operational decisions. Recently, special context problems have also been explored using DRL, including ride-hailing with electric vehicles (Kullman et al., 2021), ridesharing in SAMS (Guo and Xu, 2022), and meta-learning for transferable SAMS solutions (Gammelli et al., 2022).

The current study proposes an approach with several important features that advance the existing state of the research. First, it solves the problem using a single RL agent to model the centralized decision-making of a SAMS operator, which contrast much of the existing literature. Most studies use MARL (Holler et al., 2019; Li et al., 2019; Oda and Joe-Wong, 2018; Singh et al., 2021) or do not integrate repositioning and assignment decisions together (Fluri et al., 2018; Gammelli et al., 2022, 2021; Pavone et al., 2012). Second, the proposed approach ensures that the problem size does not increase with the size of the vehicle fleet, but only with the spatial disaggregation of the service area. While most RL approaches significantly degrade as the problem size increases relative to optimization-based methods, the proposed approach in this study continues to significantly outperform an optimization-based method at scale. Third, the problem formulation allows relocating vehicles to be assigned to passenger requests during repositioning. This feature both adds realism (real-world fleet operators will almost certainly allow for this) and improves system performance. Finally, the learning approach jointly learns the request arrival process and the traveler-vehicle assignment process, thus allowing for an integrated solution framework for efficient centralized decision-making. In fact, this last contribution enables the first two contributions—single-agent RL and a solution method that is independent of fleet size and user requests.

### 3 Notation and Problem Definition

This paper considers a case where a SAMS central operator controls a fleet of autonomous vehicles (AVs) denoted  $V = \{1, 2, \dots, |V|\}$  to serve trip requests from users  $R = \{1, 2, \dots, |R|\}$  that arrive dynamically over time. The problem is restricted to a finite horizon of time  $T = [0, t^*]$  and a pre-defined service area to which all events and decisions are constrained.

Each trip request has a request time  $t_r, \forall r \in R$  when the request is made and becomes known to the operator, which is also the earliest and desired pick-up time. Travelers cannot schedule rides

for future times. At time  $t \in T$  only requests made prior to or at  $t$  are known, forming the set of known requests:  $R_t = \{r \in R | t_r \leq t\} \subseteq R$ . Each request includes pick-up and drop-off locations, denoted  $o_r$  and  $d_r$ , respectively. We assume traveler requests cannot be canceled and will wait indefinitely.

The SAMS operator has full control over the fixed-size homogeneous AV fleet  $V$ . The full notation for the system's components and their characteristics is shown in

Table 1. We assume AVs do not need to refuel within the analysis period, so the operator makes two types of operational decisions: passenger-vehicle matching (primary decisions) and vehicle relocation (secondary decisions).

In primary decision-making, referred to as the matching or assignment problem, the operator aims to minimize operational costs and maximize customer service quality, measured via fleet miles travelled and traveler wait times, respectively. The operator cannot reject traveler requests but optimizes how and when to serve them. We do not allow shared rides, dropping, switching, or hopping of requests. In this problem, we assume the AVs will:

- maintain at most one request match at any given time,
- start travelling towards the passenger's pick-up location immediately after a match is made
- transport travelers directly to their drop-off locations, without detours or stops,
- spend a short but non-negligible amount of time during passenger boarding and alighting,
- be considered available if they have no request match at a given time.

In secondary decision-making, the vehicle repositioning problem entails choosing where to direct idle vehicles. The operator's goal remains to improve operational efficiency and improve service quality. Hence, idle vehicle relocation occurs to support the primary decisions by anticipating where and when vehicles will be needed for assignment. Relocating AVs are considered available in the primary decision stage. In vehicle repositioning, we assume AVs will:

- be directed to relocate to a new region, but not their current region,
- relocate to the new region's centroid,
- start travelling towards the destination immediately after directed to relocate, without any detours or stops.

In addition to the requests, fleet, and operator, we define the service area such that all location-related attributes of travelers and AVs have to be within the service area. While locations are considered throughout the service area continuously, we introduce a spatial disaggregation of the area into sub-areas to be used in defining the repositioning problem. The service area is modeled as a rectangular polygon, separated into a finite set  $A$  of rectangular polygon sub-areas. The full notation is presented in

Table 1, along with descriptions and any predefined (or assumed) characteristics of subareas.

This study focuses on the secondary decision problem, i.e., idle AV repositioning to improve the overall system efficiency and quality of service. The goal is to solve the AV repositioning problem for a system with a given assignment policy. In this setting, the secondary decision-making has to anticipate both the changes in the system due to incoming ride requests and those due to new AV-request assignments. The assignment problem for primary decisions is solved according to approaches presented in (Hyland and Mahmassani, 2018). Then, we pose the rebalancing problem as a Markov Decision Process (MDP) and solve it using reinforcement learning techniques. Though we separate the primary and secondary decisions into two problems, we present both problem formulations since the secondary decisions should account for the effects of future primary decisions as they are enabled by the rebalancing decisions.

Table 1. System Notation, Definitions and Characteristics

	Notation and Definition	Characteristics and Properties
Requests / Passengers	$s_r(t) \forall t \in T, r \in R$ : State of a request $r$ at time $t$	$s_r(t) \in \{0, 1, 2, 3, 4\}$ denoting unrequested, unassigned, assigned, in-vehicle and served requests respectively. <ul style="list-style-type: none"> <li><math>s_r(t) \in \{1, 2, 3, 4\} \forall t \in T, r \in R_t</math></li> <li><math>s_r(t) = 0 \forall r \in R, t &lt; t_r</math> at the request time <math>t = t_r</math>, the state is fixed s.t. <math>s_r(t_r) = 1 \forall r \in R</math></li> <li>a request's state numeric value is monotone increasing over time, i.e., if <math>t_1 &gt; t_2</math> then <math>s_r(t_1) \geq s_r(t_2) \forall r \in R</math></li> </ul>
	Subsets of requests: $R_U(t)$ Unassigned $R_A(t)$ Assigned $R_{IV}(t)$ In-vehicle $R_S(t)$ Served	$R_U(t) = \{r \in R_t   s_r(t) = 1\}; R_A(t) = \{r \in R_t   s_r(t) = 2\};$ $R_{IV}(t) = \{r \in R_t   s_r(t) = 3\}; R_S(t) = \{r \in R_t   s_r(t) = 4\}$ Collectively exhaustive: $R_U(t) \cup R_A(t) \cup R_{IV}(t) \cup R_S(t) = R_t \forall t \in T$ Mutually exclusive: $R_i(t) \cap R_j(t) = \emptyset \forall i \neq j \in \{U, A, IV, S\} \forall t \in T$
	$w_r(t) \forall t \in T, r \in R_t$ : elapsed wait time for request $r \in R_t$ at time $t$	$w_r(t) = \begin{cases} t - t_r & \text{if } s_r(t) \leq 2 \\ t'_r - t_r & \text{otherwise} \end{cases}$ , where $t'_r$ denotes the pick-up time for request $r$ if $s_r(t) > 2$ : $t'_r = \max(t \in T   s_r(t) \leq 2)$
	$p_r(t) \forall t \in T, r \in R$ : position of request $r$ at time $t$	request positions are the passengers' physical locations on a Manhattan plane; the position is fixed to the pick-up location (origin) $o_r$ before the request time $p_r(t) = o_r \forall r \in R, t \leq t_r$
Vehicle Fleet	$q_v(t) \forall t \in T, v \in V$ : state of the vehicle over time	$q_v(t) \in \{1, 2, 3, 4\}$ denoting AVs that are idle, assigned but unoccupied (en-route passenger pick-up), occupied (en-route drop-off), and relocating, respectively For $t_1$ and $t_2$ two consecutive points in time: <ul style="list-style-type: none"> <li><math>q_v(t_1) = 1 \Rightarrow q_v(t_2) \in \{1, 2, 4\}</math>, i.e., an idle AV can remain idle or change state to en-route pick up or relocating</li> <li><math>q_v(t_1) = 2 \Rightarrow q_v(t_2) \in \{2, 3\}</math> i.e., an AV en-route pick-up can remain in that state or change to en-route drop-off</li> <li><math>q_v(t_1) = 4 \Rightarrow q_v(t_2) \in \{1, 2, 4\}</math> i.e., a relocating AV can continue relocating, or change state to idle or en-route pick-up</li> </ul>
	Subsets of vehicles: $V_I(t)$ Idle AVs $V_P(t)$ En-route pick-up $V_D(t)$ En-route drop-off $V_R(t)$ Relocating	$V_I(t) = \{v \in V   q_v(t) = 1\}; V_P(t) = \{v \in V   q_v(t) = 2\}$ $V_D(t) = \{v \in V   q_v(t) = 3\}; V_R(t) = \{v \in V   q_v(t) = 4\}$ Collectively exhaustive: $V_I(t) \cup V_P(t) \cup V_D(t) \cup V_R(t) = V \forall t \in T$ Mutually exclusive: $V_i(t) \cap V_j(t) = \emptyset \forall i \neq j \in \{I, P, D, R\} \forall t \in T$
	$l_v(t) \forall t \in T, v \in V$ : vehicle $v$ 's location at time $t$	Locations are the vehicles' physical locations on a Manhattan plane
Regions	$k \in A$ : sub-areas in the set of sub-areas $A$	Regions are non-overlapping: $k_1 \cap k_2 = \emptyset \forall k_1 \neq k_2 \in A$ Regions cover the entire service area of possible locations for vehicles and requests: $l_v(t) \in \bigcup_{k \in A} k \forall v \in V, t \in T; p_r(t) \in \bigcup_{k \in A} k \forall r \in R, t \in T$



### 3.1 AV-Request Assignment Problem Formulation

The primary decision, AV-request matching, is defined as a stochastic sequential optimization problem. The goal is to find an optimal policy  $\pi$  from the set of all policies  $\Pi$  to optimize the expectation of a cost function  $C(\cdot)$  as follows:  $\min_{\pi \in \Pi} \mathbb{E}^\pi \sum_{t=0}^T C(S_t, X^\pi(S_t))$ .  $S_t$  denotes the system state at time  $t$ , and  $X^\pi(S_t)$  is policy  $\pi$ 's decision function given state  $S_t$ . The decision variables are  $x_t = x_{rv}(t)$  denoting the assignment of open traveler request  $r \in R$  to AV  $v \in V$  at time  $t$  and the function  $X^\pi(S_t) \rightarrow x_t$  for policy  $\pi$  determines the decision variable values. We assume that the evolution of the system state from time  $t$  to  $t + 1$ , (i.e., system dynamics) is a function of  $S_t$ , the decision  $x_t$  and external information  $W_{t+1}$  that includes the arrival of new travel requests with  $r_t \in (t - 1, t]$ . The external information is unknown and a random variable, hence the system state evolves probabilistically:  $S_{t+1} = P(S_t, x_t, W_{t+1})$  and the objective function includes an expectation  $\mathbb{E}^\pi(\cdot)$ .  $S_t$  consists of: the traveler requests' states  $\{s_r(t) \forall r \in R_t\}$ , positions  $\{p_r(t) \forall r \in \{R_U(t), R_A(t)\}\}$ , elapsed wait times  $\{w_r(t) \forall r \in \{R_U(t), R_A(t)\}\}$ , the AVs' states  $\{q_v(t) \forall v \in V\}$  and locations  $\{l_v(t) \forall v \in V\}$ . It includes binary indicator variables  $\{y_{rv}(t) \forall r \in \{R_U, R_A\}, v \in V\}$  equal to 1 if request  $r$  is currently assigned to AV  $v$ .

The policy we use to address the sequential matching problem is to solve an AV-request assignment problem at various decision epochs over the analysis period. In each decision epoch, we consider subsets of requests and vehicles for assignment, denoted  $R'$  and  $V'$ , respectively. Specifically, we consider the unassigned requests,  $R' = R_U$  and the idle and relocating vehicles  $V' = V_I \cup V_R$ , for assignment. Let  $d_{rv}(t)$  denote the distance between the pickup location  $o_r$  for traveler  $r \in R$  and the location  $l_v(t)$  of vehicle  $v \in V$  at time  $t$ . The problem is formulated in two ways, according to (Hyland and Mahmassani, 2018). First, if the number of requests is greater than the number of AVs available, i.e.,  $|R'| > |V'|$ :

$$\min_{x_{rv}} \sum_{r \in R'} \sum_{v \in V'} (d_{rv} x_{rv} - \alpha w_r x_{rv}) \quad (1)$$

s.t.

$$\sum_{v \in V'} x_{rv} \leq 1 \quad \forall r \in R' \quad (2)$$

$$\sum_{r \in R'} x_{rv} = 1 \quad \forall v \in V' \quad (3)$$

$$x_{rv} \geq 0 \quad \forall r \in R', v \in V' \quad (4)$$

Second, if the number of requests is less than or equal to the AVs available, i.e.,  $|R'| \leq |V'|$ :

$$\min_{x_{rv}} \sum_{r \in R'} \sum_{v \in V'} d_{rv} x_{rv} \quad (5)$$

s.t.

$$\sum_{v \in V'} x_{rv} = 1 \quad \forall r \in R' \quad (6)$$

$$\sum_{r \in R'} x_{rv} \leq 1 \quad \forall v \in V' \quad (7)$$

$$x_{rv} \geq 0 \quad \forall r \in R', v \in V' \quad (8)$$

In the first case, the objective function in Equation (1) has two terms representing the total distance between travelers and AVs assigned and the elapsed wait time for assigned travelers. The weight  $\alpha$  scales and converts the wait time units into the distance equivalent. The objective

function in the second case in Equation 5 minimizes the overall distance between AVs and requests in the assignment. The constraints are parallel but differ in the two cases based on whether there is an ‘excess’ of trip requests or vehicles.

### 3.2 AV Repositioning Problem Formulation

The secondary decision, AV repositioning, is defined as a fully observed Markov Decision Process (MDP)  $\mathcal{M}_{reb}(\mathcal{S}^{reb}, \mathcal{A}^{reb}, P^{reb}, r^{reb})$  defined by the state space, action space, probabilistic dynamics, and reward function, respectively. The aim is to learn a behavioral policy that will select the desired rebalancing of vehicles between sub-areas. We use a discretized spatial representation for this secondary decision problem. The service area is represented as a graph  $\mathcal{G}(\mathcal{V}, \mathcal{E})$  where the vertices  $\mathcal{V}$  are the sub-areas  $A$  as defined in Table 1 represented by their centroids, and the edges  $\mathcal{E}$  represent shortest paths connecting the sub-areas’ centroids as an approximation of travel times between the sub-areas.  $\mathcal{G}$  is a complete directed graph, where  $\mathcal{E} = \{(i, j) \mid \forall i, j \in \mathcal{V}\}$ . In the discrete time horizon  $T$ , the state  $S^{reb}(t) \in \mathcal{S}^{reb}$  contains the information needed to determine the rebalancing strategy, the action  $A^{reb}(t) \in \mathcal{A}^{reb}$  is a behavior policy that describes a distribution of the vehicles over the edges.  $P^{reb}$  describes the dynamics of the system through a conditional probability distribution:  $P^{reb}(S^{reb}(t+1) \mid S^{reb}(t), A^{reb}(t))$ , and  $r : \mathcal{S} \times \mathcal{A} \rightarrow \mathbb{R}$  defines a reward function.

We solve this problem using reinforcement learning with a single agent choosing a multi-dimensional action  $A^{reb}(t) \in \mathcal{A}^{reb}$  and learning a policy that defines a distribution over possible actions given states  $\pi(A^{reb}(t) \mid S^{reb}(t))$ .

The multi-dimensional action is  $A^{reb}(t) = [A_{ij}^{reb}(t)] \forall (i, j) \in \mathcal{E}$ , where  $A_{ij}^{reb}(t) \in [0, 1]$  defines the percentage of currently idle vehicles at node  $i \in \mathcal{V}$  to be rebalanced towards node  $j \in \mathcal{V}$ , and  $\sum_{j \in \mathcal{V}} A_{ij}^{reb}(t) = 1 \forall i \in \mathcal{V} t \in T$ . From this distribution, the number of rebalancing vehicles is calculated as  $\rho_{ij}(t) = \lfloor A_{ij}^{reb}(t) \omega_i(t) \rfloor$  where  $\lfloor \cdot \rfloor$  is the floor function ensuring  $\rho$  is an integer and less than or equal to the available number of vehicles  $\omega_i(t)$ , i.e., the number of idle vehicles at node (sub-area)  $i$  and time  $t$ .

$S^{reb}(t)$  contains knowledge of the graph  $\mathcal{G}(\mathcal{V}, \mathcal{E})$  along with vertex and edge level information by means of a feature matrix  $\mathbf{N}$  and adjacency matrix  $\mathbf{M}$ . The feature matrix  $\mathbf{N}_t$  is a collection of the following information: number of currently idle vehicles in each region  $[[v \in V_I(t) \mid l_v(t) \in i] \mid \forall i \in \mathcal{V}]$ , number of vehicles currently relocating towards each region:  $[[v \in V_R(t) \mid d_v(t) \in i] \mid \forall i \in \mathcal{V}]$ , number of vehicles arriving with passengers to each region:  $[[v \in V_D(t) \mid d_r \cdot y_{rv}(t) \in i] \mid \forall i \in \mathcal{V}]$ .  $\mathbf{M}$  describes the graph  $\mathcal{G}(\mathcal{V}, \mathcal{E})$  via the edge lengths, i.e., pairwise travel times between the sub-areas’ centroids. We assume fixed shortest-path travel times on a Manhattan grid, but the formulation allows for a time-varying  $\mathbf{M}(t)$  as well. Additionally, it contains the number of originating passenger requests at each region for a specified number of time periods  $w_i(t) = [[r \in R \mid o_r \in i, r_t \in [t - \delta, t]]]$ . The input information could contain expected future demand as predictions or rely on past demand observations to make inferences.

$P^{reb}$  describes the evolution of the state over time, including the evolution of the travel demand patterns and the influence of primary and secondary decisions on the future state elements. The demand evolution is stochastic and independent of the relocation and assignment decisions, hence  $P^{reb}$  is a stochastic process.

The reward function is defined from the perspective of the operator to capture the system efficiency and service quality, aiming to approximate the mean passenger waiting time. However, since the mean is not a cumulative summative value, we express the reward at each time step via a negative (penalty) term for passenger waiting times and a positive term for the number of served passengers, with weights on each term. The reward at time  $t$ , with a time-discretization interval  $\delta$ , is computed as:

$$r(t) = -\omega \cdot \delta \cdot (|R_U(t)| + |R_S^\delta(t)|) + \sigma |R_S^\delta(t)| \quad (9)$$

where  $R_U(t)$  is the set of unassigned requests (i.e., waiting passengers) at time  $t$  and  $R_S^\delta(t)$  is the set of requests served in the last  $\delta$ -duration interval:  $R_S^\delta(t) = \{R_S(t)\} \setminus \{R_S(t - \delta)\}$ . Thus,  $(|R_U(t)| + |R_S^\delta(t)|)$  is the number of passengers that have been waiting during the last  $\delta$ -duration interval with a total wait time of  $\delta \cdot (|R_U(t)| + |R_S^\delta(t)|)$  since time  $t - \delta$ , while  $|R_S^\delta(t)|$  is the number of served requests since time  $t - \delta$ . The parameters  $\omega$  and  $\sigma$  are the weights that scale the two parts of the reward function that have different units.

Since the effects of repositioning decisions on the system state and performance are not immediate, the goal is to optimize the operational decisions over a given time horizon. The agent learns to maximize a cumulative reward resulting from all states and actions, instead of immediate reward caused by one action at one state. The evolution of the system, or what the RL literature calls the trajectory, is the sequence of states and actions for the specified time horizon  $T$ :  $\mathcal{T} = (S^{reb}(0), A^{reb}(0), S^{reb}(1), A^{reb}(1), \dots, S^{reb}(t^*), A^{reb}(t^*))$ . Given the stochastic system dynamics,  $\mathcal{T}$  with the policy  $\pi$  has the distribution:

$$p_{\pi(\mathcal{T})} = d_0(s_0) \prod_{t=0}^{t^*} \pi(A^{reb}(t) | S^{reb}(t)) p^{reb}(S^{reb}(t+1) | S^{reb}(t), A^{reb}(t)) \quad (10)$$

The RL objective  $J(\pi)$  in Equation 11 is to maximize the expected cumulative reward under this distribution:

$$\max_{\pi} \mathbb{E}_{\mathcal{T} \sim p_{\pi(\mathcal{T})}} \left[ \sum_{t=0}^{t^*} \gamma(t) r(S^{reb}(t), A^{reb}(t)) \right] = \max_{\pi} J(\pi) \quad (11)$$

where  $\gamma(t) \in (0, 1] \forall t \in T$  is a discount factor that can vary over time if needed, and  $r(S^{reb}(t), A^{reb}(t))$  is the reward function. In our formulation,  $\gamma(t)$  is constant and there are no notions of cost for the service to the operator, nor earnings from serving demand to define the reward function via costs or profits. Instead, the reward weights are determined so that  $J(\pi)$  approximates the negative mean request wait time, i.e.,  $-\frac{(\sum_{r \in R} w_r(t^*))}{|R|}$ . The exact values for  $\omega$  and  $\sigma$  can be derived via

$$\sum_{t=0}^{t^*} r(S^{reb}(t), A^{reb}(t)) = -\omega \cdot \sum_{r \in R} w_r(t^*) + \sigma |R_S(t^*)| \equiv -\frac{\sum_{r \in R} w_r(t^*)}{|R|} \quad (12)$$

which results in

$$\omega = \frac{\sigma |R_S(t^*)| \cdot |R| + \sum_{r \in R} w_r(t^*)}{|R| \sum_{r \in R} w_r(t^*)}. \quad (13)$$

## 4 Solution Approach

The solution method employs an operational strategy to solve the SAMS problems defined in the previous section paired with an agent-based simulation tool for evaluation. The simulation tool models the operation of a SAMS fleet, including generating or obtaining demand for rides from

external data, employing approaches for assignment and repositioning of the AVs, and simulating the movement of vehicles as they fulfill passenger pick up, drop off, and strategic repositioning assignments. The simulation tool used in this study has been presented and used in several studies in the literature (Dandl et al., 2019; Hyland et al., 2021, 2019; Hyland and Mahmassani, 2018).

#### 4.1 Agent-Based Simulation Framework

The agent-based simulation tool is used to read and update the position and status of AVs and passengers in a time-driven manner within a SAMS system. The general steps taken by the simulation are outlined in Figure 1, similar to that in Dandl et al. (2019) with some key differences. Firstly, the movement of all vehicles towards their destinations is shown as a single step, since they are executed in the same manner and at the same step in simulation, regardless of the nature of their next location (i.e., pick-up, drop-off, or relocation destination). Secondly, the operational decision procedure chooses the next operational decision for the system, whether that be vehicle assignment or repositioning. If both actions are performed, they could be performed jointly or sequentially, and not necessarily with the same time interval. In this study, the methodology for the operational decision step is presented in the next two sections.

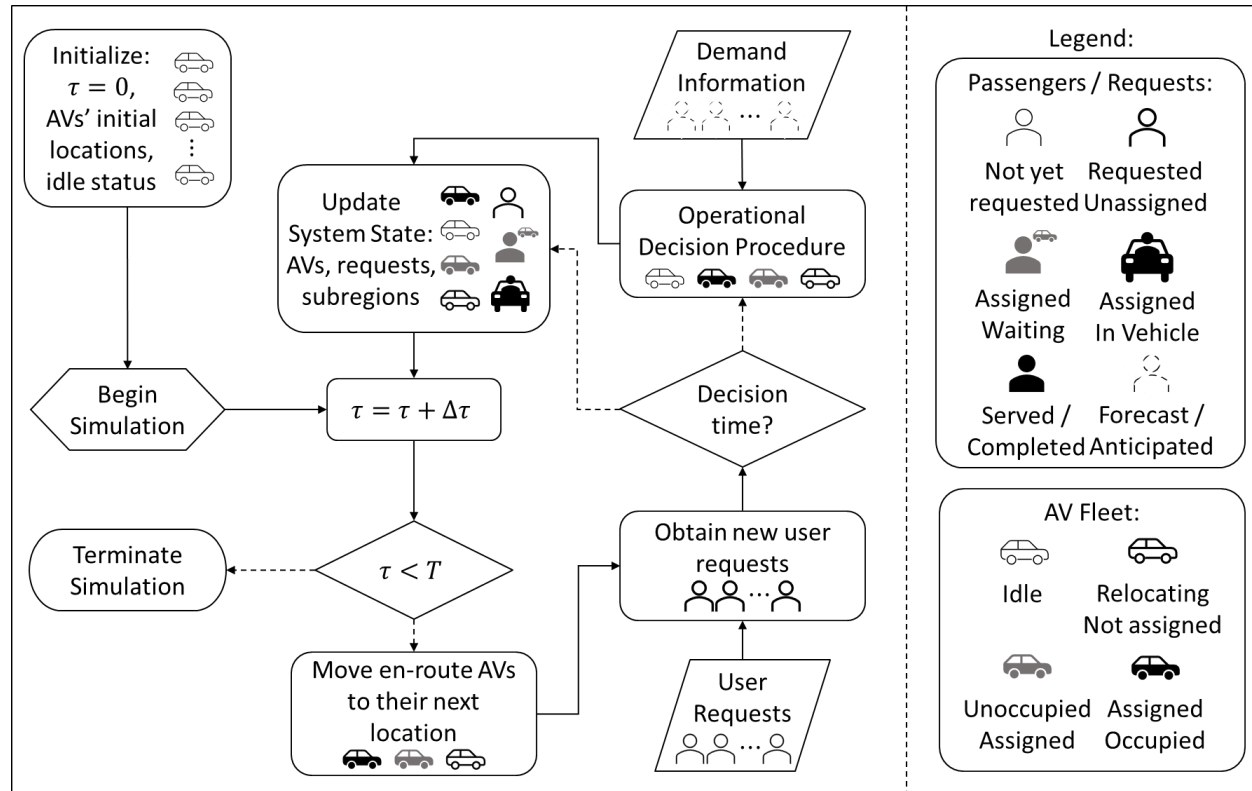


**Figure 1. Agent-based SAMS simulation framework**

In this simulation framework, the current time  $\tau$  is updated by the simulation time step  $\Delta\tau$  and the simulation runs for a simulation period  $T$ . During the times when  $\tau \leq T$  the simulation performs a sequence of tasks. First, all en-route AVs are moved closer to their next location. For occupied vehicles, this would typically be the drop-off destination, for unoccupied vehicles that are assigned this would be a request pick-up location, and for relocating unassigned vehicles it would be the relocation position. It should be noted that other types of next locations may exist in

special cases such as those allowing shared rides or passenger hopping. Second, the simulation obtains new requests that have occurred during the time interval  $\Delta\tau$  since the last time step. Next, the simulation checks if the current time  $\tau$  is also a decision time. If so, the simulation calls the operational decision procedure, otherwise it continues to update the system state. The operational decision procedure is left broad here and can be specified based on the operational needs for a specific problem. For example, it may include assignment of vehicles to new requests and/or the assignment of vehicles to relocate to new positions. The procedure can also accommodate special-case decision-making, such as the decision to assign another request to a vehicle if shared rides are allowed, or to free up a vehicle by allowing a passenger to ‘hop’ to another shared ride. To perform this task the simulation may also admit additional information regarding the demand if needed, such as spatio-temporal demand forecasts. Updating the system state is performed to account for the new information received and/or operational decisions made during the current time step. This involves updating the status of all passengers or requests and the AV fleet that took place due to time passing (for example, passengers that were waiting are now in-vehicle) or due to operational decisions (for example, an idle vehicle is now en route to pick up a passenger). Here the terms passenger and request are used interchangeably due to the specific problem considered in this study. However, the simulation framework allows for requests to include multiple passengers, which may be relevant for shared-ride cases where vehicle occupancy should also be tracked. Finally, the simulation terminates if  $\tau \geq T$ .

## 4.2 Two-Part Operational Framework

The two-part SAMS operational framework, summarized Figure 2, solves of the two decision problems, where the “SAMS System” contains all steps from the agent-based simulation except the operational decision procedure. The external demand generation is an input to the SAMS system, and the system delivers and receives information to and from the two decision-making components. Notably the two operational decision modules do not communicate with one another, except by observing one another’s impacts on the system state.

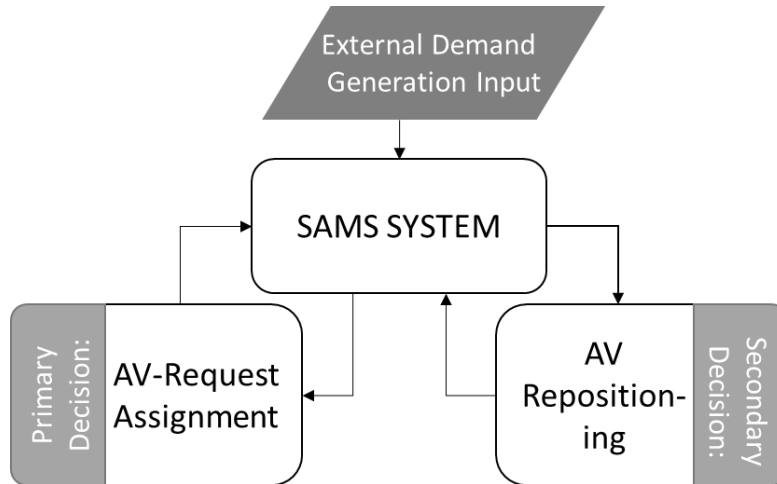


**Figure 2. Two-Part Operational Framework for the SAMS System**

### 4.2.1 AV-Request Assignment Approach

The approach for the AV-request assignment problem is adopted from (Hyland and Mahmassani, 2018) based on the subsets  $R' = R_U$  and  $V' = V_I \cup V_R$  of requests and vehicles considered for

assignment, respectively. We consider the two applicable approaches from (Hyland and Mahmassani, 2018), and adjust them so that  $V'$  includes idle and relocating, instead of just idle vehicles.

- Strategy A sequentially assigns travelers FCFS to the nearest idle AV or relocating vehicle.
- Strategy B solves the optimization problems presented previously to simultaneously determine the assignment between the requests in  $R' = R_U$  and vehicles in  $V' = V_I \cup V_R$ .

#### 4.2.2 AV Repositioning Approach: Advantage Actor-Critic (A2C) Reinforcement Learning (RL) Agent

Having defined the SAMS rebalancing problem as an MDP, we solve it using an RL algorithm that follows a standard learning loop: the agent interacts with the environment  $\mathcal{M}_{reb}$  by applying a behavior policy  $\pi(A^{reb}|S^{reb})$ , where it observes the state  $S^{reb}(t)$ , chooses an action  $A^{reb}(t)$  and then observes the next state  $S^{reb}(t+1)$  together with scalar reward feedback  $r(t) = r(S^{reb}(t), A^{reb}(t))$ . The procedure repeats and the agent uses the observed transitions  $(S^{reb}(t), A^{reb}(t), S^{reb}(t+1), r(t))$  to update the policy.

With the goal of maximizing the cumulative reward, we solve this problem by estimating the gradient of the objective  $J(\pi)$  so that the learning process is solved by an approximate gradient ascent approach. We parametrize the policy  $\pi$  by a parameter vector  $\theta$  so that it is given by  $\pi_\theta(A^{reb}(t)|S^{reb}(t))$ . The gradient is expressed as:

$$\nabla_\theta J(\pi_\theta) = \mathbb{E}_{\mathcal{T} \sim p_{\pi_\theta}(\tau)} \left[ \sum_{t=0}^{t^*} \gamma^t \nabla_\theta \log \pi_\theta(A^{reb}(t)|S^{reb}(t)) \hat{A}(S^{reb}(t), A^{reb}(t)) \right] \quad (11)$$

with the advantage estimator:

$$\hat{A}(S^{reb}(t), A^{reb}(t)) = \sum_{t'=t}^{t^*} \gamma^{(t'-t)} r(S^{reb}(t'), A^{reb}(t')) - b(S^{reb}(t)) \quad (12)$$

where  $b(S^{reb}(t))$  is the estimator for the state value function (Mnih et al., 2016):

$$V^\pi(S^{reb}(t)) = \mathbb{E}_{\mathcal{T} \sim p_{\pi_\theta}(\tau|S^{reb}(t))} \sum_{t'=t}^{t^*} \gamma^{(t'-t)} r(S^{reb}(t'), A^{reb}(t')) \quad (13).$$

An Advantage Actor-Critic (A2C) algorithm will be used to solve this problem by finding the policy  $\pi_\theta(A^{reb}(t)|S^{reb}(t))$  and the value function estimator  $V(S^{reb}(t))$ . A2C is an actor-critic (AC) method, a type of temporal-difference (TD) learning. TD methods learn from raw experience, without a model of the environment dynamics, which is an important aspect of the SAMS problem. AC methods have these characteristics, but they also separately parametrize the policy and the value function, so they are composed of a policy structure that selects the actions, known as the *actor*, and an estimated value function that evaluates (or criticizes) the actions, known as the *critic*. The *critic* learns and criticizes the policy followed by the *actor*, where the critique is parametrized via a TD error (Barto et al., 1995; Sutton and Barto, 2015).

A2C methods employ a *critic* that estimates the advantage function  $\hat{A}(S^{reb}(t), A^{reb}(t))$  to perform gradient ascent on the objective function  $J(\pi_\theta)$  (Mnih et al., 2016). The A2C process for the SAMS rebalancing problem is shown in Figure 3, where the environment contains all remaining components of the operational framework: the SAMS System, the primary decision, and the demand input. The A2C agent interacts with this environment by drawing observations of

the environment state, observed by the *actor* and *critic* components. The *actor* develops a policy to choose an action feeding back into the SAMS system which implements changes resulting from this action. Based on the updated environment, a reward is observed by the *critic* component. The *critic* computes the advantage of the action and feeds it back to the *actor* so it can update the policy.

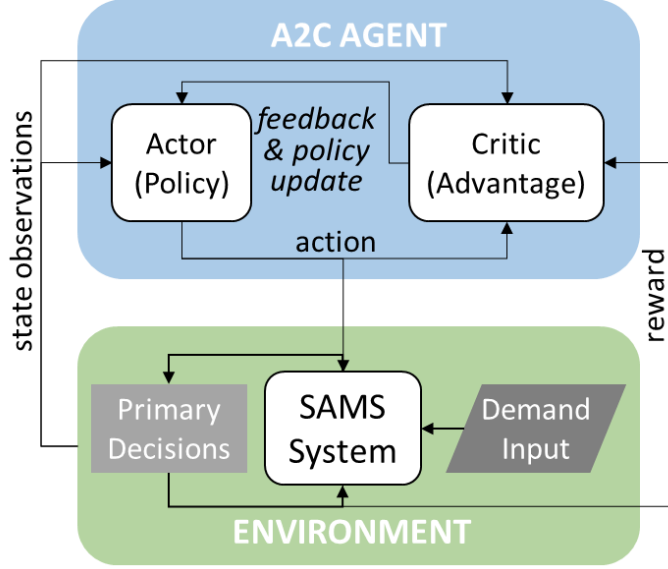


Figure 3. A2C agent with a SAMS environment

The A2C agent parametrizes the policy and the value-function estimator via deep neural network architectures for the actor and critic components, respectively. The policy defines the rebalancing action  $A^{reb}(t) = [A_{ij}^{reb}(t)] \forall (i, j) \in \mathcal{E}$ , where  $A_{ij}^{reb}(t) \in [0, 1]$  defines the percentage of currently idle vehicles at node  $i \in \mathcal{V}$  to be rebalanced towards node  $j \in \mathcal{V}$ , and  $\sum_{j \in \mathcal{V}} A_{ij}^{reb}(t) = 1 \forall i \in \mathcal{V} t \in T$ . For  $\pi_{\theta}(A^{reb}(t) | S^{reb}(t))$  to define a valid probability density over actions, the output of the policy network represents the concentration parameters  $\alpha$  of a Dirichlet distribution  $Dir(\cdot)$ , such that  $A^{reb}(t) \sim Dir(A^{reb}(t) | \alpha) = \pi_{\theta}(A^{reb}(t) | S^{reb}(t))$ . The neural network for the actor consists of a graph attention network (GAT) layer, followed by four layers of graph convolutional neural network (GCN) with skip-connections and Rectified Linear Unit (ReLU) activations. Its output is aggregated across neighboring nodes using a permutation-invariant sum-pooling function and passed to three multi-layer perceptron (MLP) layers to produce the Dirichlet concentration parameters. The value function is defined using a similar architecture, where the main difference is a global sum-pooling performed on the output of the graph convolution so that it computes a single value function estimate for the entire network.

## 5 Numerical Experiments

### 5.1 Study Sites and Data

#### 5.1.1 New York City Taxi Demand Data

To implement, test and evaluate the proposed approach, this study uses New York City (NYC) yellow and green taxi trip record data made publicly available by the NYC Taxi and Limousine

Commission (TLC), as collected and provided by technology providers authorized under the Taxicab & Livery Passenger Enhancement Programs (NYC Taxi & Limousine Commission, 2022). For this study, one month of trip data were accessed from April 2016 for the island of Manhattan.

The following transformations and assumptions were made on the trip data for the purposes of using it in the form of time-dependent passenger origin-destination pairs within the simulation framework presented in Section 4.1. Firstly, the simulation assumes that user requests are made at the trip start times, according to the original data set, and the pick-up and drop-off locations for each trip are the origin and destination points for the corresponding request in the simulation. Secondly, in the data pre-processing stage, all zero-distance trips were removed, i.e., trips where the origin and destination were at the same location.

Some summary statistics of the data are presented in Table 2, including the number of trips per day, hourly trips, and average trip distance. The average, standard deviation, minimum and maximum for these quantities were computed over all days in the data and only for weekdays separately. Overall, daily trips average at over 329,000 trips per day and over 13,000 trips per hour, across the full set of days considered in this data set. On average trip distances over a full day of trips were 2.841 km (i.e., 1.765 miles). It should be noted that these summary statistics differ slightly from those presented by Dandl et al. (2019) despite using the same data set, due to the pre-processing step of removing zero-distance trips, which accounted for close to 1,000 trips in each day's data on average.

**Table 2. NYC Taxi Data Summary Statistics for April 2016**

	All Days			Weekdays		
	Daily Trips	Average hourly trips	Trip Distance [km]	Daily Trips	Average hourly trips	Trip Distance [km]
Mean	329,838.2	13,743.26	2.841	326,691.5	13,612.14	2.788
St. dev.	27,227.58	1,134.482	0.0961	22,653.05	943.8771	2.672
Min	27,3754	11,406.42	2.672	273,754	11,406.42	2.844
Max	38,5946	16,081.08	3.072	367,412	15,308.83	0.041

The distribution of the trips throughout the day is another important component in understanding the potential needs for fleet management and operations. The number of hourly trip requests for each of the 24 hours in a day for all days of April 2016 used in this study are presented in Figure 4. The trip numbers for the 21 weekdays are shown with orange-shaded solid lines (best viewed in color), while those for the 9 weekend dates are plotted in the blue shaded dashed lines.



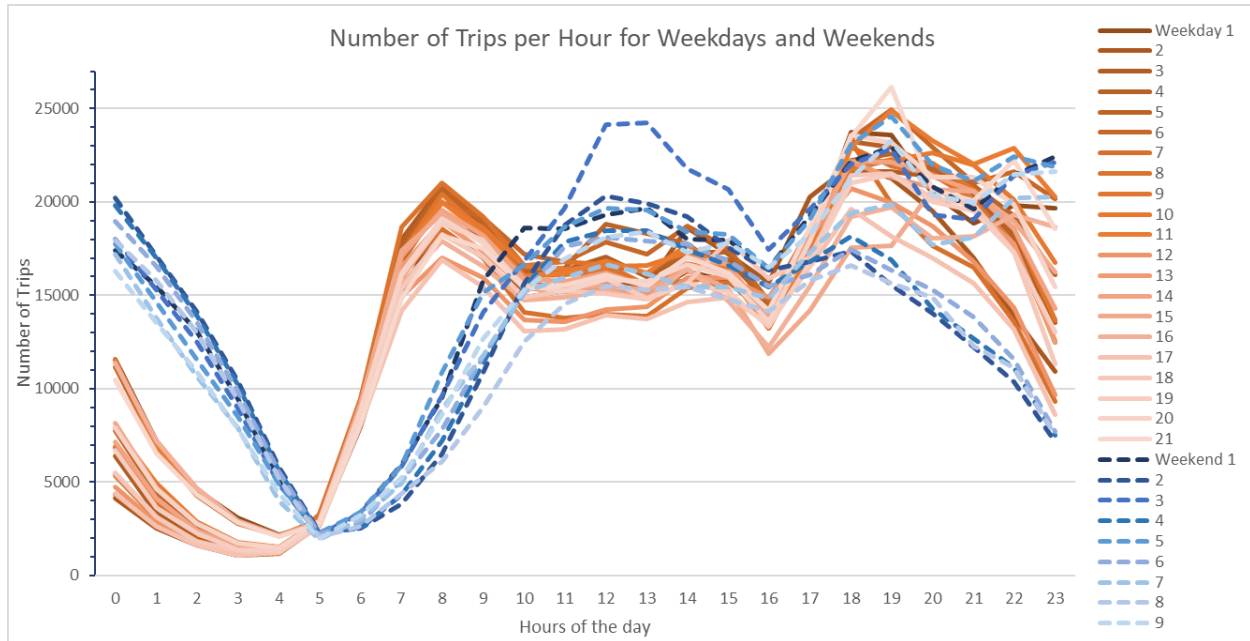


**Figure 4. Temporal Variations in Demand Across Hours of the Day and Days in the Month**

Figure 4 shows that there are distinct temporal peaks and dips in demand during the day. On weekdays, early morning trips, between 2 and 5 am, can range from 1000 to 4000 trips per hour and reach values from 15,000 to 22,000 hourly trips for the morning peak hours between 6 and 9 am. On the other hand, weekend demand patterns have more early morning trips and a morning peak period that starts later, after around 7 am, and stretches into the afternoon. The high numbers of trip requests during the morning and evening peak periods indicate the potential for strategic vehicle repositioning.

To better understand the spatial distribution of trips as well as differences between weekday and weekend patterns, Figure 5 shows density plots for trip pick-up and drop-off locations for weekdays and weekends in April 2016, obtained using the kernel density analysis function in ArcGIS. The density is represented with a color scale ranging from red (high) to green (low) density.

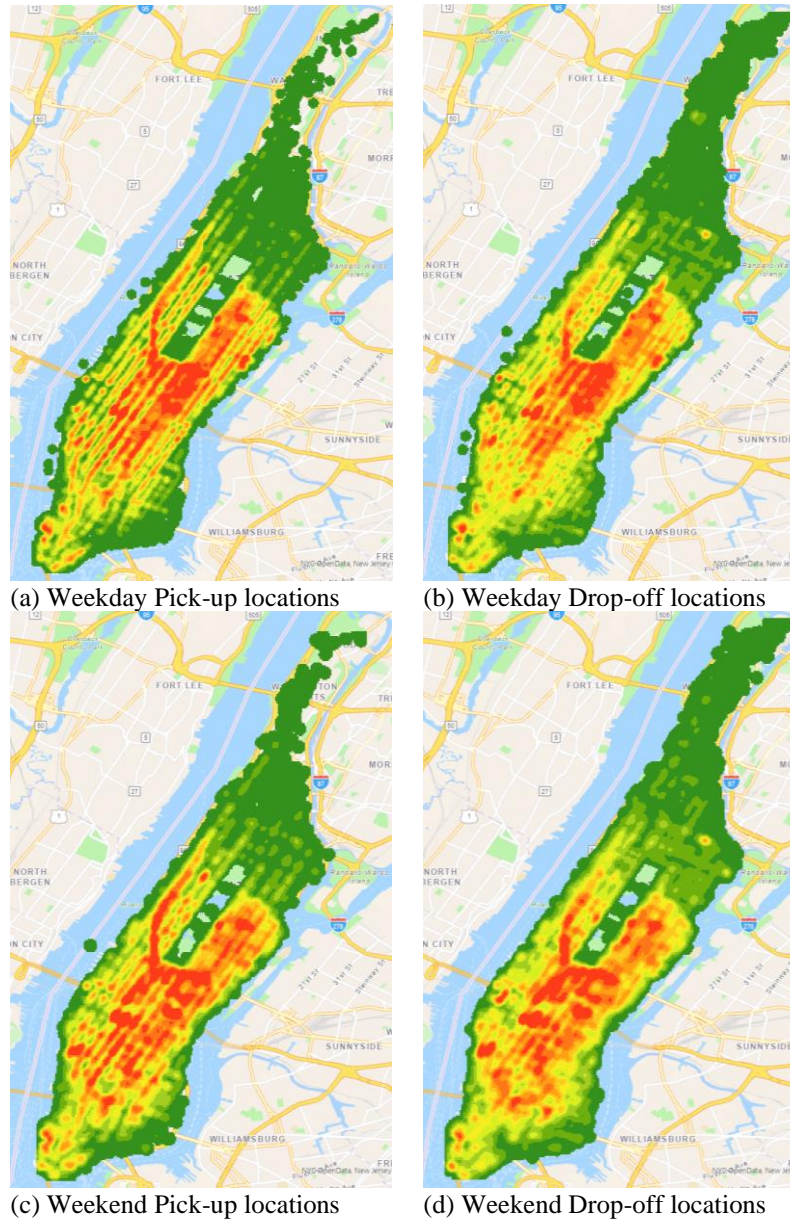


**Figure 5. Taxi data trip pick up and drop off density for weekdays (a-b) and weekends (c-d). Red and green areas represent locations of high and low density, respectively.**

### 5.1.2 New York City Spatial Regions

To accommodate for the fact that the simulation tool simulates vehicle movements using Manhattan distance and only along the x-axis and y-axis, the coordinate system was rotated so that movements along the x-axis and y-axis approximately align with the Manhattan street network grid, similarly to the approach taken by Dandl et al. (2019). The service area was specified as a rectangle around the island of Manhattan, and similar to the approach in (Dandl et al., 2019) we divide the island into 16 approximately square sub-areas to be used for the vehicle repositioning problem. The centroids for the sub-areas were computed as demand centroids, instead of area-based centroids.

## 5.2 Experimental Design

At the training stage, we implement two versions of the A2C AV repositioning approach (A2C-AVR) with different observations of demand: A2C-AVR(A) which only observes past demand, and A2C-AVR(B) which receives predictions of future demand. The future demand predictions are based on the demand forecast model presented in (Dandl et al., 2019), which assumes that demand is generated by a Poisson distribution process and aims to model the rate of new user requests  $\lambda$  in the Poisson distribution. Observing predicted demand as part of the state for the RL agent is similar to the approach in (Gammelli et al., 2021). Hence, comparing the performance of A2C-AVR(A) and A2C-AVR(B) allows us to determine if a model that only observes past demand performs as well as a model with future demand predictions. We also implement an optimization-based rebalancing (OBR) approach for vehicle rebalancing according to (Dandl et al., 2019), as a baseline for comparison purposes. The OBR method is tested with the same predictions of future demand as those in the A2C-AVR-(B) model.

**Table 3. Simulation parameters, values, and corresponding scenario settings and models**

Parameter	Value	Scenario Setting	Scenario	Model
Vehicle speed	5 m/s (11 mph)	--		--
Drop-off time	15 s	--		--
Pick-up time	45 s	--		--
Simulation time step	15 s	--		--
Inter-decision interval	30 s	--		OBR
Assignment decision interval	30 s	--		A2C-AVR
Repositioning decision interval	300 s (5 min)	--		A2C-AVR
Prediction horizon	30 min	--		OBR
Prediction horizon	90 min	--		A2C-AVR(B)
Demand prediction interval	300 s (5 min)	--		OBR, A2C-AVR(B)
AV-Request assignment	Strategy A	Strategy A	1, 3, 5, 7	--
	Strategy B	Strategy B	2, 4, 6, 8	--
Demand fraction	0.1	--		--
AV fleet size	600	--		--
Simulation start time	5 a.m.	AM Peak	1-4	--
	3 a.m.	Full Day	5-8	--
Simulation end time	12:59 p.m.	AM Peak	1-4	--
	11:59 p.m.	Full Day	5-8	--
Days of the week	Weekdays	Weekday	1, 2, 5, 6	--
	Weekends	Weekend	3, 4, 7, 8	--

Table 3 shows the simulation parameters and settings for the numerical experiments used to define experiment scenarios. Parameters where the scenario setting or model are not specified apply to all cases. The scenario settings result in a total of 8 scenarios labelled 1-8 in the table, and defined as follows:

- Scenario 1: AM peak period, weekdays, assignment strategy A
- Scenario 2: AM peak period, weekdays, assignment strategy B
- Scenario 3: AM peak period, weekend, assignment strategy A
- Scenario 4: AM peak period, weekend, assignment strategy B
- Scenario 5: Full day period, weekdays, assignment strategy A
- Scenario 6: Full day period, weekdays, assignment strategy B
- Scenario 7: Full day period, weekend, assignment strategy A
- Scenario 8: Full day period, weekend, assignment strategy B

The RL models A2C-AVR(A) and A2C-AVR(B) were trained with scenario 1, where the reduced demand allows for stochasticity in demand patterns observed by the agent in each episode (i.e., simulation period). During training, the models' convergence is quantified via loss values on the policy and value function estimation, presented in Figure 6. Both models' loss functions converge to zero, but the A2C-AVR(B) model converges more quickly and obtains values closer to zero. Thus, A2C-AVR(A) was trained for an additional 2,000 episodes to achieve similar convergence. The corresponding reward function values are shown in Figure 7, smoothed with a sliding window of 50 episodes, to make the overall trend more apparent. Model version (B) achieves higher reward function values not attained by version (A) even with additional training.

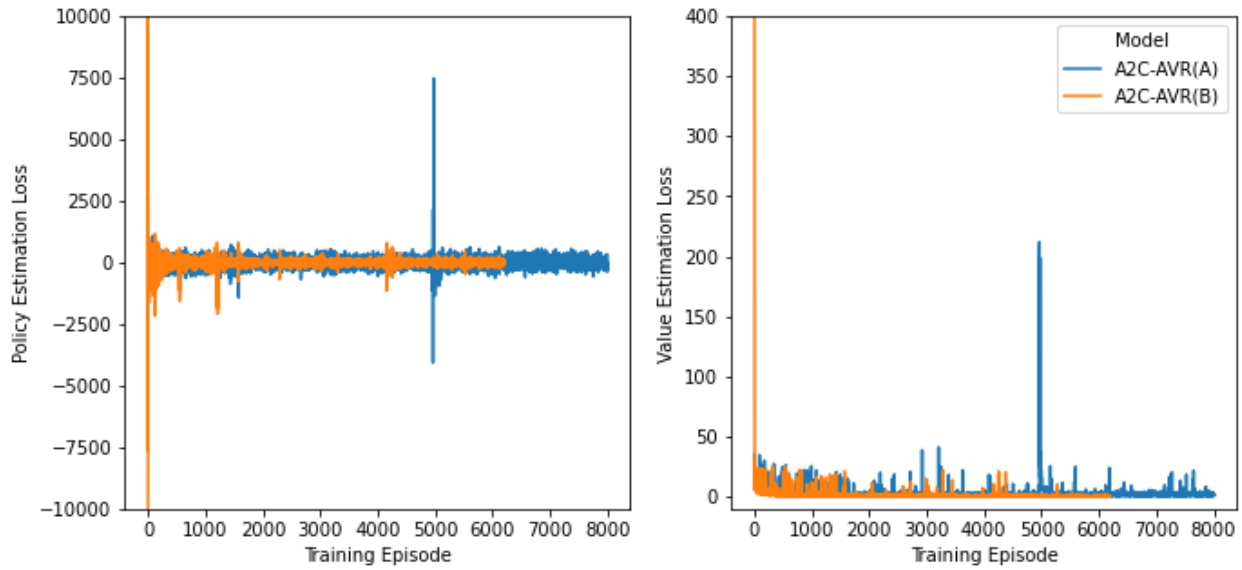


**Figure 6. Policy and value function estimation loss across the training episodes for models A2C-AVR(A) and A2C-AVR(B)**

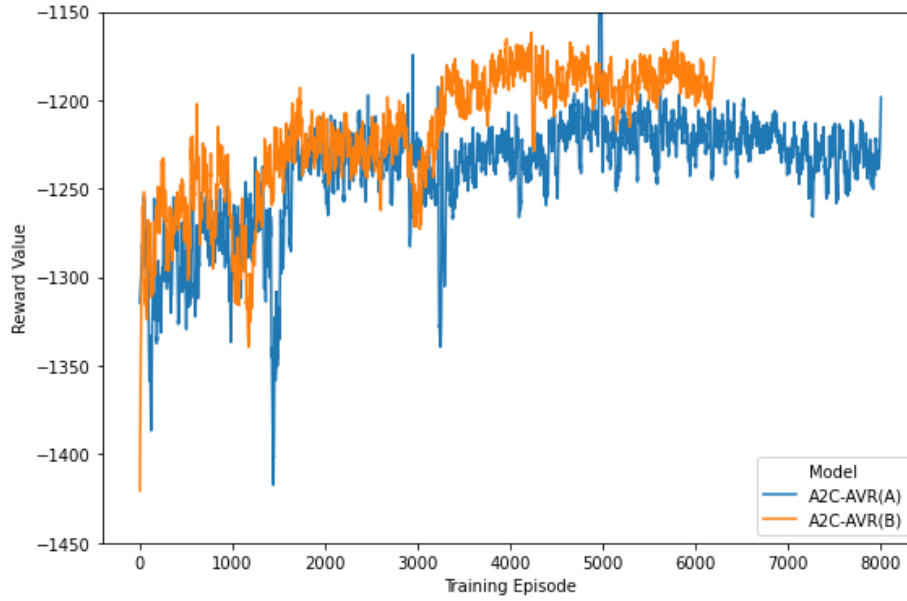


Figure 7. Training reward function values across for models A2C-AVR(A) and A2C-AVR(B)

### 5.3 Results and Analysis

Models A2C-AVR(A) and A2C-AVR(B), trained only on scenario 1, were tested on all eight scenarios to evaluate their performance across unseen cases and demand patterns. The main experimental results include the mean and standard deviation of request wait times in seconds. Additionally, the percent empty fleet distance and fleet utilization are presented, where the latter is the percent of time that vehicles spent travelling as opposed to idling. These performance metrics are shown for all models across the 8 scenarios in Table 4 and visualized in Figures 8 through 12.

Table 4. Average values of performance measures across 8 scenarios for 3 models

Scenario	Mean request wait time			Request wait time standard deviation		
	A2C-AVR(A)	A2C-AVR(B)	OBR	A2C-AVR(A)	A2C-AVR(B)	OBR
1	100.62	100.76	239.10	72.52	72.86	163.24
2	84.33	84.78	231.89	47.22	47.78	147.67
3	100.19	98.57	239.86	72.71	70.00	164.95
4	83.67	84.56	233.33	46.78	47.78	149.78
5	119.86	112.86	225.57	149.95	131.57	146.38
6	88.11	85.33	202.00	57.44	50.89	123.78
7	108.76	102.71	224.14	112.00	96.48	145.14
8	86.67	84.22	201.22	55.22	50.00	123.00
Scenario	Percent empty distance			Percent fleet utilization		
	A2C-AVR(A)	A2C-AVR(B)	OBR	A2C-AVR(A)	A2C-AVR(B)	OBR
1	53%	53%	52%	63%	63%	44%
2	66%	66%	52%	62%	62%	32%
3	53%	53%	49%	63%	63%	44%
4	66%	66%	49%	62%	62%	32%
5	53%	52%	48%	72%	71%	49%
6	54%	54%	48%	73%	72%	47%
7	52%	52%	48%	71%	71%	49%
8	54%	54%	48%	72%	72%	47%

Figure 8 shows that A2C-AVR approaches result in significantly lower mean wait times compared to the OBR approach, by more than 50% in all but one scenario, pointing to significant improvements in the system’s service quality when employing the A2C approaches. Mean wait times for the A2C-AVR(A) and A2C-AVR(B) approaches are close to one another, with more significant differences observable in the full day scenarios (5 through 8) ranging from 2.8% to 5.8% of additional wait time reductions achieved with approach (B) relative to approach (A). Nevertheless, the performance of A2C-AVR(A) is very close to that of A2C-AVR(B), demonstrating that the A2C-based repositioning approach can learn relatively well without any demand predictions. These results also demonstrate the transferability of the A2C-AVR models to unseen scenarios, such as the weekend demand patterns and the full-day cases.

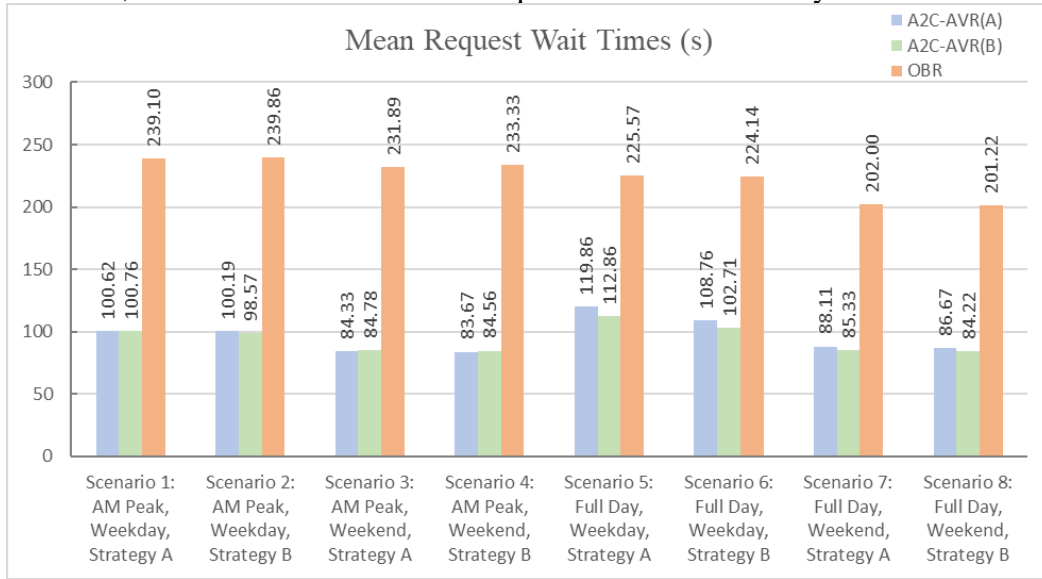


**Figure 8. Mean request wait times across testing episodes, for the 3 models and 8 scenarios**

In Figure 9 we see the standard deviation of passenger wait times for the 8 scenarios and all three models. Both A2C-AVR models result in lower standard deviation of wait times compared to the OBR approach for all scenarios except scenario 5. In all AM peak scenarios, A2C-AVR approaches consistently achieve low wait time standard deviation. In the full day scenarios 5 through 8, the wait time standard deviations are closer to those achieved by the OBR approach, and in scenario 5 they were higher, showing that the A2C-AVR approach has higher variability of wait times for previously unseen scenarios. It is interesting to observe that the A2C-AVR approaches transfer well to weekend scenarios, such as 3 and 4, and seem to have better transferability to full-day weekend scenarios (7 and 8) compared to full-day weekday scenarios (5 and 6). For some understanding of the potential causes of these differences, we can return to the demand patterns for weekdays and weekends as observed in the data, shown in Figure 4. One possibility is that the full-day weekend cases seem to have a single peak period, which is similar to the AM peak period, though longer in duration. On the other hand, the full-day weekday scenarios have a second PM peak period that is not seen in training and could thus lead to increased standard deviation of waiting times as observed in scenarios 5 and 6 in Figure 9.



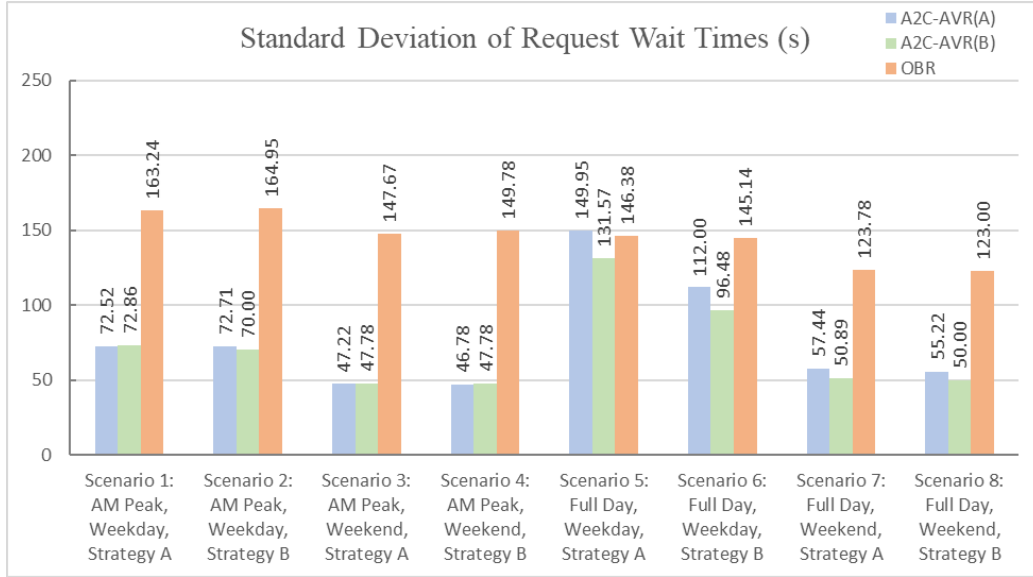


**Figure 9. Standard deviation of request waiting times across testing episodes, for the 3 models and 8 scenarios**

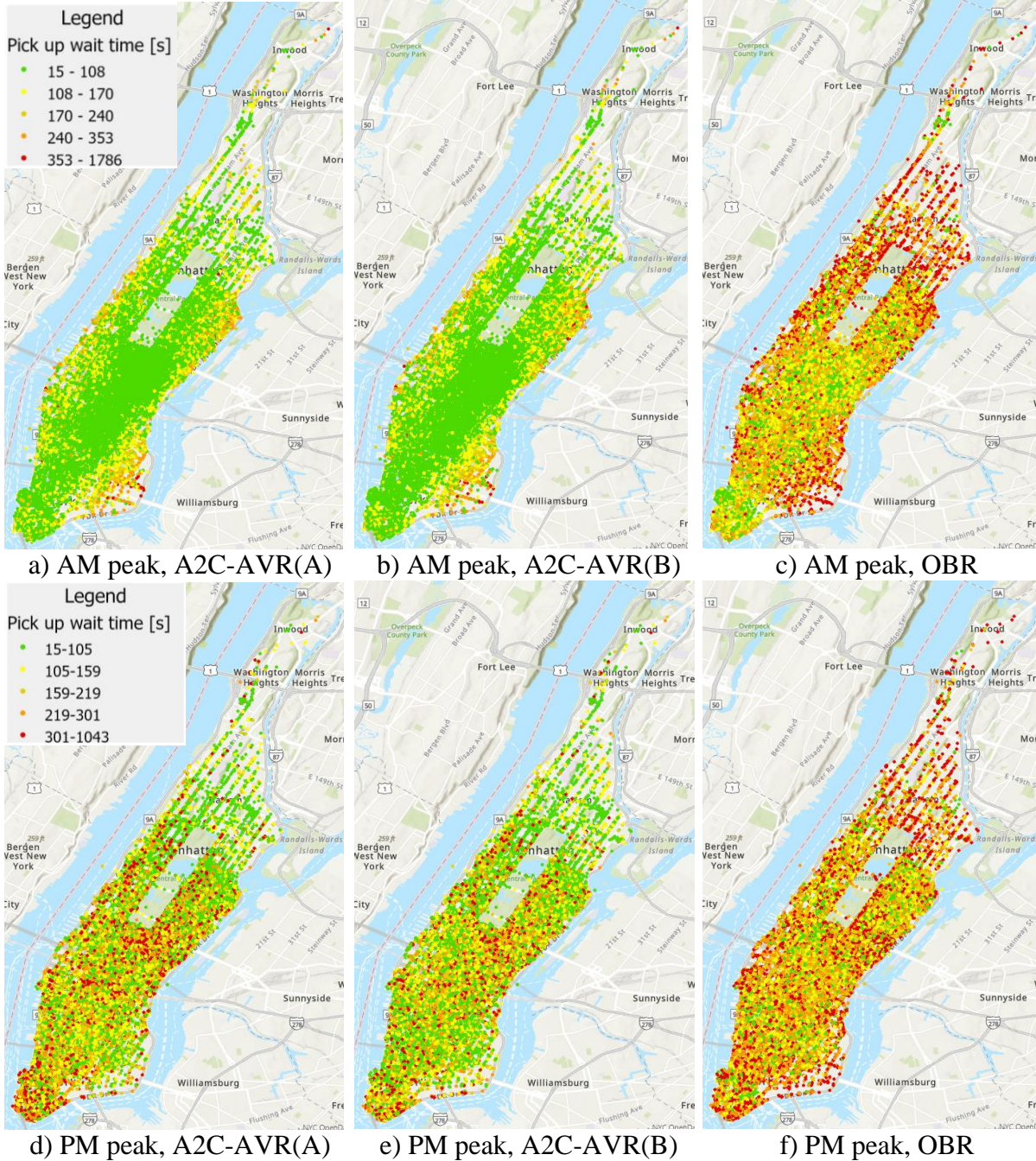
To gain further understanding of the variability of waiting times across the service area and during different times of day, the waiting times for the peak periods of scenario 5 (weekdays) and scenario 7 (weekends) are shown in Figures 10 and 11, respectively. The results were visualized using ArcGIS, plotting the requests as points at their pick-up locations, where the color indicates the average pick-up wait times in seconds. The graduated colors separate the waiting times into quantiles determined based on the observed wait times across the three models for a given scenario and time period. For example, in the legend for Figures 10 a), b) and c) the red-colored points indicate waiting times above the 80<sup>th</sup> percentile, while the green-colored points are waiting times below the 20<sup>th</sup> percentile across all three models.

Comparing Figures 10 a) b) and c) for the weekday AM peak period, the wait times for the two A2C-AVR models are significantly lower and exhibit less variation than those for the OBR model. However, comparing those to the results in Figure 10 d), e) and f) for the weekday PM peak period, there is significantly more variation in wait times for all three models. While A2C-AVR models perform better than the OBR approach in terms of overall waiting times, the variation in wait times during the PM peak period is notably higher compared to the results seen in Figure 10 a) and b).

On the other hand, the results in Figure 11 for the weekend scenario, scenario 7, show more consistency in the model performance between the AM and PM peak periods, and illustrate the improvements achieved by both A2C-AVR models compared to the OBR approach. These results demonstrate that the A2C-AVR models, trained on a weekday AM peak period scenario, transfer better to full-day weekend relative to weekday PM peak scenarios. This indicates that the models would likely benefit from additional training with weekday PM peak period demands.

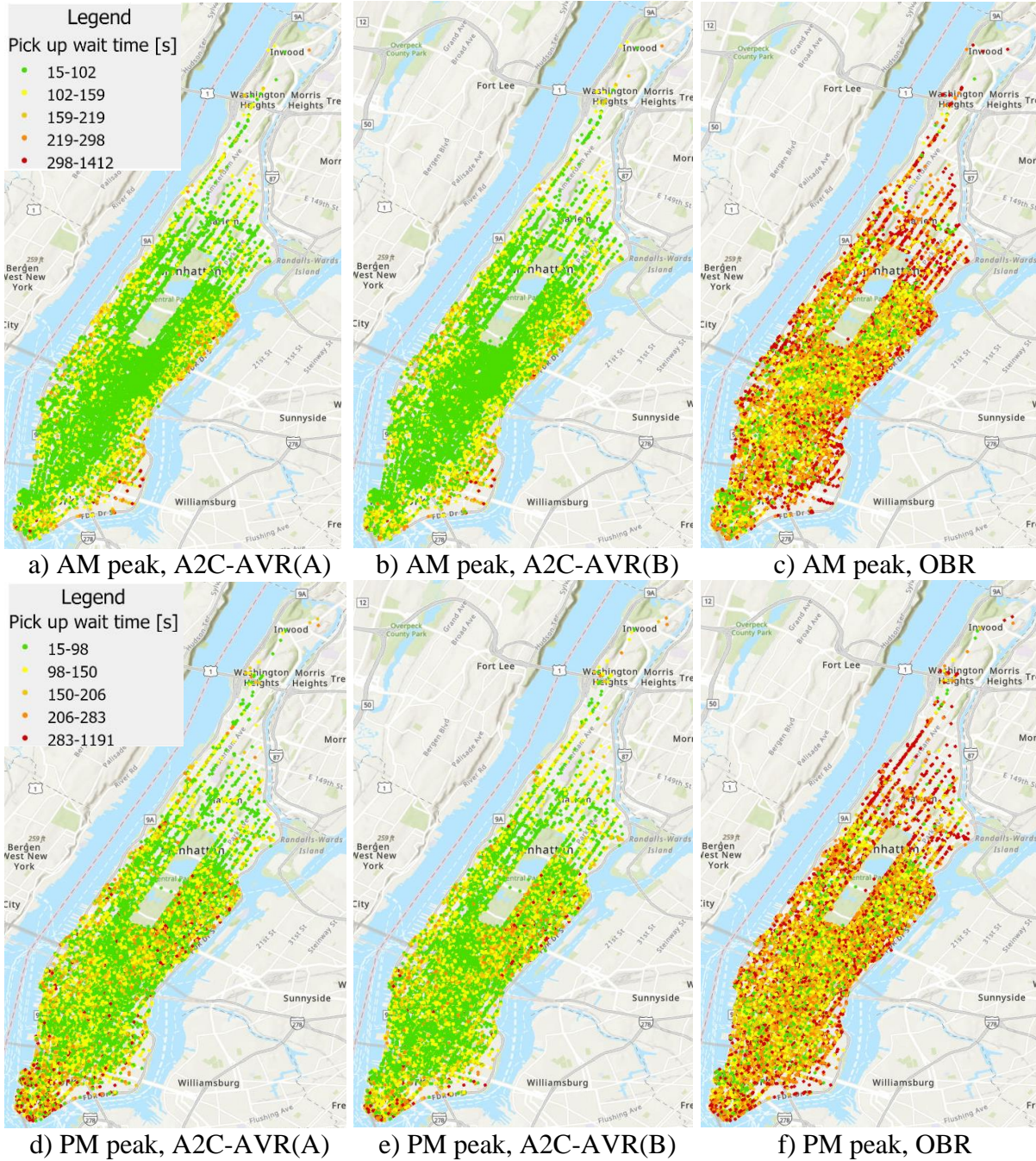
Further considering these results, it is interesting to note that even when there can be an increase in variation of the wait times resulting from the A2C-AVR models, as observed in Figure 10 d) and e), the variation is evenly distributed throughout the service area and there does not appear to be a significant imbalance between service quality provided to different sub-areas or neighborhoods. This is in contrast with the results for the OBR approach, where in Figure 10 c) there are distinct areas such as midtown, east side, and lower Manhattan experiencing low wait times in contrast to neighborhoods such as Harlem experiencing high wait times. While equal distribution of service quality may need to be further quantified and measured, these results

indicate the potential for improving equity and fairness in SAMS services using the A2C-AVR approach. This is a particularly surprising finding, given that neither the reward function in the learning-based repositioning model nor the objective function in the optimization-based assignment model incentivize an equitable distribution of vehicles or wait times. This surprising and interesting finding requires further examination as the results may not hold across other metrics, and the results may not generalize or transfer to non-Manhattan networks.



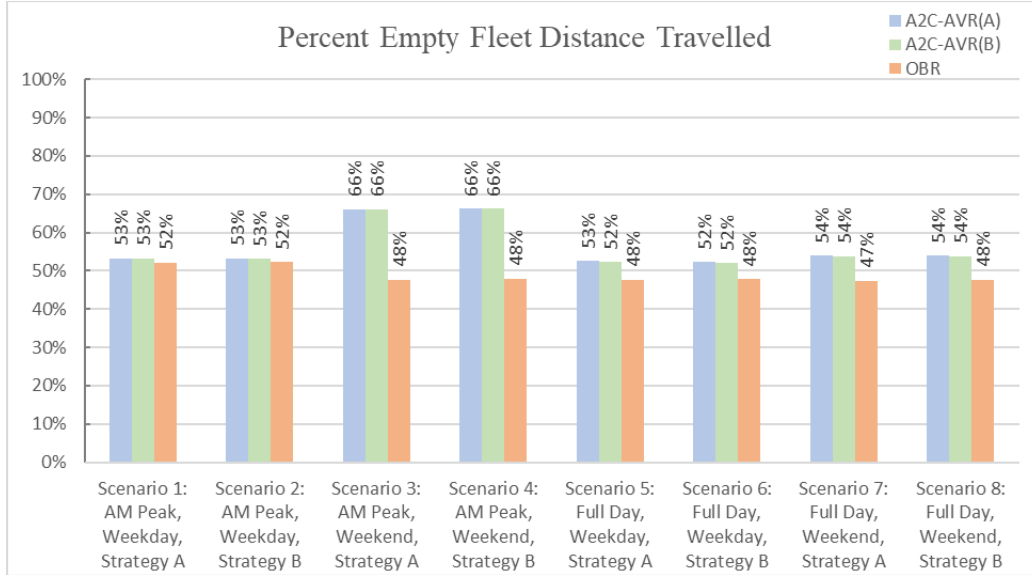
**Figure 10. Request wait times at pick up locations for scenario 5, during the AM peak period (a-c) and PM peak period (d-f) for the models A2C-AVR(A) in a) and d), A2C-AVR(B) in b) and e), and OBR in c) and f)**





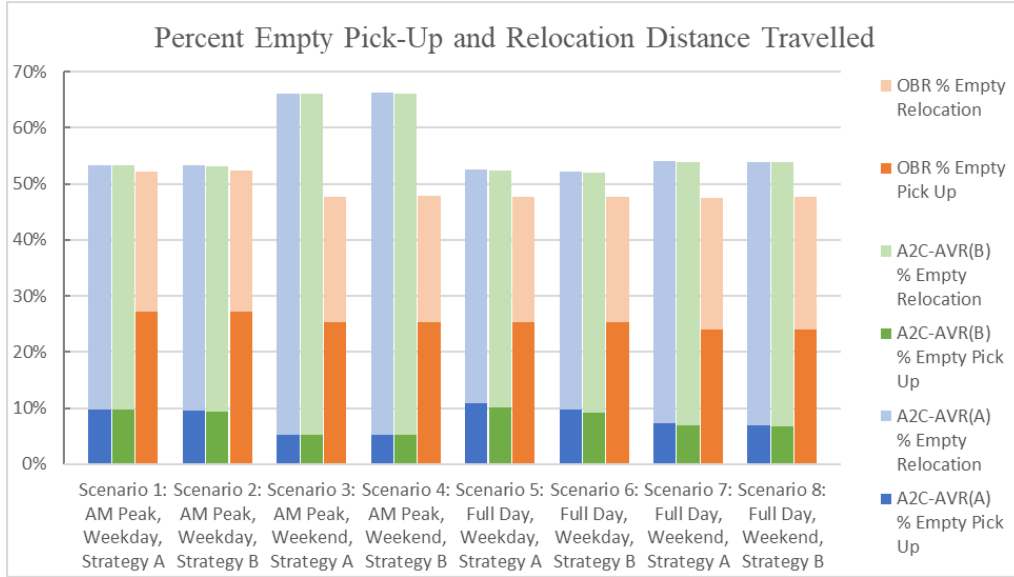
**Figure 11. Request wait times at pick up locations for scenario 7, during the AM peak period (a-c) and PM peak period (d-f) for the models A2C-AVR(A) in a) and d), A2C-AVR(B) in b) and e), and OBR in c) and f)**

Figure 12 shows the percent of empty fleet distance travelled, which is calculated as the distance travelled while vehicles were unoccupied as a percentage of the total fleet distance travelled. The percent empty fleet distance travelled in most scenarios slightly higher using A2C-AVR models compared to the OBR approach, with the increase ranging from 1 to 7 percentage points in all but two scenarios. In scenarios 3 and 4, the tradeoff between waiting times and empty fleet distance travelled is especially apparent. While the percent empty distance was 37.5% (i.e., 18 percentage points) higher than with the OBR approach, mean request wait times were 68% lower, as seen in Figure 8. It is interesting to note that there is no observable difference in the percent empty fleet distance between models (A) and (B), even though model (B) performed better in terms of wait times.



**Figure 12. Empty distance travelled as percent of all fleet distance travelled, averaged across testing episodes, for the 3 models and 8 scenarios**

Since empty fleet miles can be due to repositioning and passenger pick up, Figure 13 shows the percent empty distance travelled by vehicles for each of the two purposes. It is important to observe that the OBR approach has a relatively even split of empty distance due to relocation and passenger pick-up. On the other hand, with the A2C-AVR approaches most of the empty distance is travelled due to relocation and the distance travelled due to pick up is significantly reduced. Most other operational policies in the literature with repositioning, have a higher proportion of empty miles stemming from empty pickup trips than empty repositioning trips. While it may seem counterintuitive, this indicates that the repositioning decisions are accurate in placing the vehicles close to upcoming demand so that the pick-up distance can be significantly reduced. In fact, these results demonstrate that the short passenger wait times achieved by A2C-AVR approaches are due to the vehicles' proximity to upcoming demand which is successfully achieved by the relocation algorithm. In contrast, the results for the OBR approach indicate that even with the repositioning scheme, vehicles travel just as much for passenger pick up as they did during the repositioning. Moreover, this illustrates how the A2C-AVR can significantly reduce user wait times compared to the OBR approach. In the OBR approach, the user has to wait for the empty pickup movements, whereas users do not have to wait for empty repositioning movements.



**Figure 13. Percent empty distance travelled due to passenger pick-up and relocation averaged across testing episodes, for the 3 models and 8 scenarios**

Figure 14 shows the percent fleet utilization, i.e., the percentage of time that vehicle fleets spent travelling as opposed to idling. The A2C-AVR models result in higher fleet utilization across all scenarios, which can indicate that vehicles are travelling more than needed. However as seen in Figure 12, that is not due to significantly higher empty fleet miles travelled.

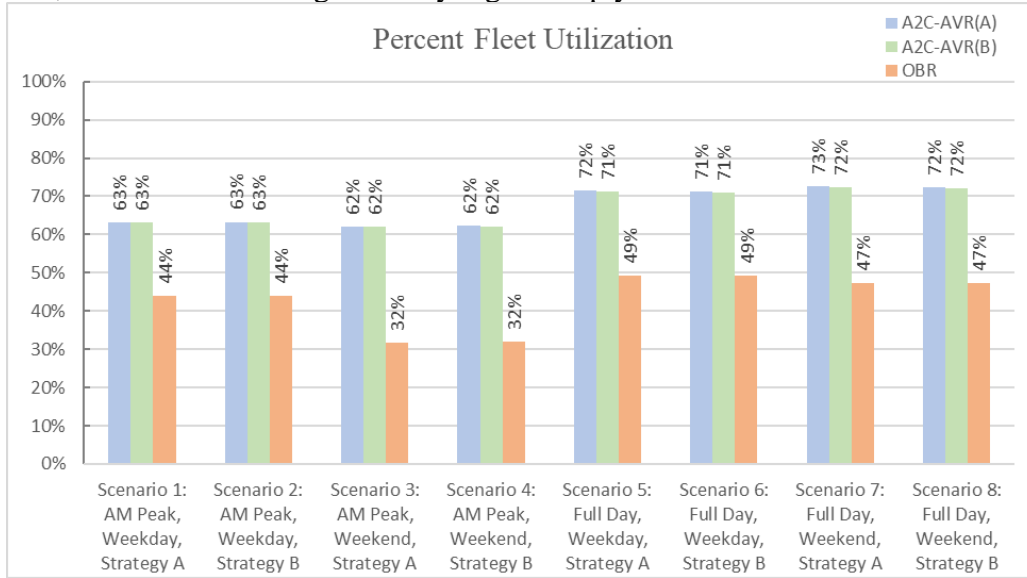


**Figure 14. Percent fleet utilization averaged across testing episodes, for the 3 models and 8 scenarios**

Overall, the experimental results indicate that the A2C-AVR approach can significantly improve system performance compared to a policy with an optimization-based approach for the repositioning problem. The gap is particularly large in terms of service quality, since the learning-based models were trained with a reward function based on waiting times. The results also demonstrate the models' transferability to full day and weekend demand patterns, despite training only on the weekday AM peak period. In the context of real-world SAMS applications, especially in a competitive market, successfully reducing the pick-up distances and corresponding request

waiting times can lead to increased market shares in cases where passengers consider and compare several service providers. Paired with an appropriate pricing strategy, the service provider can achieve a balance between the operational costs of additional empty miles travelled and users' willingness to pay for improved service quality.

## 6 Conclusion

This paper considers the operation of SAMS fleets and focuses on the problem of idle vehicle repositioning to ultimately improve system efficiency and service quality. The SAMS system is modeled from the operator's perspective, making primary request-to-AV assignment decisions and secondary repositioning decisions. We pose the secondary AV repositioning problem as an MDP that integrates with an optimization-based assignment approach for the primary assignment problem. The MDP is solved using an advantage actor critic (A2C) AV rebalancing reinforcement learning approach abbreviated A2C-AVR.

We implement two versions of the proposed approach for learning the behavioral policy for vehicle rebalancing. The first, A2C-AVR(A), observes past demands in the system and learns to anticipate future demand by also learning the underlying demand patterns, and an alternative version, A2C-AVR(B), that learns using externally supplied demand forecasts. In numerical experiments, both model versions are trained on a single scenario for a weekday AM peak period with a given assignment approach. The models are tested across 8 scenarios, including full day as well as weekend demands and an alternative assignment approach. The approaches are compared to one another and to a benchmark optimization-based rebalancing (OBR) approach across the testing scenarios. The experiments demonstrate that the A2C-AVR approaches can significantly improve mean passenger wait times relative to the OBR approach, at the expense of slightly increased percent of empty fleet miles travelled. The effectiveness of the repositioning strategy is also demonstrated by the decrease in distance travelled for passenger pick-up, showing that AVs are positioned at the right times and location where demand arises. The two A2C-AVR approaches perform comparably well across unseen scenarios, further demonstrating their transferability to cases with unseen demand patterns, extended operational periods, and changes in the AV assignment strategy. The results show opportunity for improvement in the models' performance for weekday PM peak periods. However, even in cases where some variation in wait times is observed when using the A2C-AVR approaches, they outperform the OBR approach in several aspects, including the fairness in spatial distribution of service quality, while maintaining the performance in terms of average measures of efficiency.

The paper opens opportunities for future research in the domain and extensions of the proposed approach. For example, it might be interesting to evaluate the performance of the approach with different spatial and temporal aggregation levels or different approaches for implicit or explicit demand forecasting. Other types of operator decisions can also be considered as part of the problem including shared rides, passenger hopping, and vehicle refueling or charging. Considering the observations related to equity in the distribution of service quality, especially when comparing the proposed approach to the OBR method, there is potential for future work to augment the A2C-AVR approaches for fair and equitable SAMS services.

As a final point, a large number of studies over the past decade have addressed the operational problem of a SAMS without shared rides. We believe there are two critical future research directions related to this operational problem. First, operational policies in the literature (i.e., optimization-based, reinforcement learning, approximate dynamic programming, etc.) need to be tested in the real world. While some operational policies from researchers at Didi have been tested



in their real-world ridesourcing service, their service includes human drivers who have some autonomy of critical operational decisions. Given the emergence of actual SAMS or robo-taxi services in the United States and China, where the central operator has complete control over vehicle routes, testing SAMS operational policies from the literature in these services is a critical future research direction. Second, despite multiple research groups ostensibly addressing the same real-world problem, there are no standard datasets or problem instances to compare operational policies. Moreover, the field lacks a set of standard simulators, which would go along with standard datasets and problem instances, to properly compare operational policies. Instead, each research group makes a variety of *different* simplifying assumptions when creating their own simulators. Given the importance of this research area, another critical future research direction is to create standard datasets, a large number of diverse problem instances, and a set of simulators, to allow for effective comparison of newly proposed approaches to the current state-of-the-art across a variety of scenario settings.

### **Acknowledgements**

Part of this work was supported by the Office of the Vice President for Research (OVPR) at the University of Connecticut via funding provided to the first author through the Research Excellence Program award.

## References

- Alonso-Mora, J., Samaranayake, S., Wallar, A., Frazzoli, E., Rus, D., 2017. On-demand high-capacity ride-sharing via dynamic trip-vehicle assignment, in: *Proceedings of the National Academy of Sciences of the United States of America*. National Academy of Sciences, pp. 462–467.  
[https://doi.org/10.1073/PNAS.1611675114/SUPPL\\_FILE/PNAS.1611675114.SM01.MP4](https://doi.org/10.1073/PNAS.1611675114/SUPPL_FILE/PNAS.1611675114.SM01.MP4)
- Barto, A.G., Bradtke, S.J., Singh, S.P., 1995. Learning to act using real-time dynamic programming. *Artif Intell.* [https://doi.org/10.1016/0004-3702\(94\)00011-O](https://doi.org/10.1016/0004-3702(94)00011-O)
- Chaniotakis, E., Antoniou, C., Pereira, F., 2016. Mapping Social media for transportation studies. *IEEE Intell Syst* 31, 64–70. <https://doi.org/10.1109/MIS.2016.98>
- Dandl, F., Bogenberger, K., 2019. Comparing Future Autonomous Electric Taxis With an Existing Free-Floating Carsharing System. *IEEE TRANSACTIONS ON INTELLIGENT TRANSPORTATION SYSTEMS* 20. <https://doi.org/10.1109/TITS.2018.2857208>
- Dandl, F., Engelhardt, R., Hyland, M., Tilg, G., Bogenberger, K., Mahmassani, H.S., 2021. Regulating mobility-on-demand services: Tri-level model and Bayesian optimization solution approach. *Transp Res Part C Emerg Technol* 125, 103075. <https://doi.org/10.1016/J.TRC.2021.103075>
- Dandl, F., Hyland, M., Bogenberger, K., Mahmassani, H.S., 2019. Evaluating the impact of spatio-temporal demand forecast aggregation on the operational performance of shared autonomous mobility fleets. *Transportation (Amst)* 46, 1975–1996. <https://doi.org/10.1007/S11116-019-10007-9/TABLES/2>
- Fagnant, D.J., Kockelman, K.M., 2015. Operations of Shared Autonomous Vehicle Fleet for Austin, Texas, Market. *Transportation Research Record: Journal of the Transportation Research Board* 2536, 98–106. <https://doi.org/10.3141/2536-12>
- Fagnant, D.J., Kockelman, K.M., 2014. The travel and environmental implications of shared autonomous vehicles, using agent-based model scenarios. *Transp Res Part C Emerg Technol* 40, 1–13. <https://doi.org/10.1016/J.TRC.2013.12.001>
- Federal Transit Administration, 2021. Mobility on Demand (MOD) Sandbox Program | FTA [WWW Document]. URL <https://www.transit.dot.gov/research-innovation/mobility-demand-mod-sandbox-program> (accessed 12.13.21).
- Fluri, C., Ruch, C., Zilly, J., Hakenberg, J., Frazzoli, E., Fluri, C., Ruch, C., Zilly, J., Hakenberg, J., 2018. Learning to Operate a Fleet of Cars. <https://doi.org/10.3929/ETHZ-B-000304517>
- Gammelli, D., Yang, K., Harrison, J., Rodrigues, F., Pereira, F.C., Pavone, M., 2022. Graph Meta-Reinforcement Learning for Transferable Autonomous Mobility-on-Demand. <https://doi.org/10.48550/arXiv.2202.07147>
- Gammelli, D., Yang, K., Harrison, J., Rodrigues, F., Pereira, F.C., Pavone, M., 2021. Graph Neural Network Reinforcement Learning for Autonomous Mobility-on-Demand Systems. <https://doi.org/10.1109/CDC45484.2021.9683135>
- Gueriau, M., Dusparic, I., 2018. SAMoD: Shared Autonomous Mobility-on-Demand using Decentralized Reinforcement Learning. *IEEE Conference on Intelligent Transportation Systems, Proceedings, ITSC 2018-November*, 1558–1563. <https://doi.org/10.1109/ITSC.2018.8569608>
- Guo, G., Xu, Y., 2022. A Deep Reinforcement Learning Approach to Ride-Sharing Vehicle Dispatching in Autonomous Mobility-on-Demand Systems; A Deep Reinforcement Learning

- Approach to Ride-Sharing Vehicle Dispatching in Autonomous Mobility-on-Demand Systems. <https://doi.org/10.1109/MITS.2019.2962159>
- Holler, J., Vuorio, R., Qin, Z., Tang, X., Jiao, Y., Jin, T., Singh, S., Wang, C., Ye, J., 2019. Deep reinforcement learning for multi-driver vehicle dispatching and repositioning problem. *Proceedings - IEEE International Conference on Data Mining, ICDM 2019-November*, 1090–1095. <https://doi.org/10.1109/ICDM.2019.00129>
- Hörl, S., Becker, F., Axhausen, K.W., 2021. Simulation of price, customer behaviour and system impact for a cost-covering automated taxi system in Zurich. *Transp Res Part C Emerg Technol* 123, 102974. <https://doi.org/10.1016/J.TRC.2021.102974>
- Hyland, M., Dandl, F., Bogenberger, K., Mahmassani, H., 2019. Integrating demand forecasts into the operational strategies of shared automated vehicle mobility services: spatial resolution impacts Integrating demand forecasts into the operational strategies of shared automated vehicle mobility services: spatial reso. *Transportation Letters*. <https://doi.org/10.1080/19427867.2019.1691297>
- Hyland, M., Mahmassani, H.S., 2020. Operational benefits and challenges of shared-ride automated mobility-on-demand services. *Transp Res Part A Policy Pract* 134, 251–270. <https://doi.org/10.1016/J.TRA.2020.02.017>
- Hyland, M., Mahmassani, H.S., 2018. Dynamic autonomous vehicle fleet operations: Optimization-based strategies to assign AVs to immediate traveler demand requests. *Transp Res Part C Emerg Technol* 92, 278–297. <https://doi.org/10.1016/j.trc.2018.05.003>
- Hyland, M., Yang, D., Sarma, N., (Calif.), M.T.C., Pacific Southwest Region 9 UTC, U. of S.C., University of California, I., 2021. Non-Myopic Path-Finding for Shared-Ride Vehicles: A Bi-Criteria Best-Path Approach Considering Travel Time and Proximity To Demand. <https://doi.org/10.21949/1503647>
- Hyland, M.F., Mahmassani, H.S., 2017. Taxonomy of Shared Autonomous Vehicle Fleet Management Problems to Inform Future Transportation Mobility: *Transportation Research Record: Journal of the Transportation Research Board* 2653, 26–34. <https://doi.org/10.3141/2653-04>
- Ihler, A., Hutchins, J., Smyth, P., 2006. Adaptive Event Detection with Time-Varying Poisson Processes General Terms Algorithms, in: *KDD '06: Proceedings of the 12th ACM SIGKDD International Conference on Knowledge Discovery and Data Mining*.
- Kullman, N.D., Cousineau, M., Goodson, J.C., Mendoza, J.E., 2021. Dynamic Ride-Hailing with Electric Vehicles. <https://doi.org/10.1287/TRSC.2021.1042>
- Li, M., Qin, Z., Jiao, Y., Yang, Y., Gong, Z., Wang, J., Wang, C., Wu, G., Ye, J., 2019. Efficient Rideshar-ing Order Dispatching with Mean Field Multi-Agent Reinforcement Learn-ing 11. <https://doi.org/10.1145/nnnnnnnn.nnnnnnnn>
- Maciejewski, M., Bischoff, J., Nagel, K., 2016. An Assignment-Based Approach to Efficient Real-Time City-Scale Taxi Dispatching; An Assignment-Based Approach to Efficient Real-Time City-Scale Taxi Dispatching, *IEEE Intelligent Systems*. <https://doi.org/10.1109/MIS.2016.2>
- Mnih, V., Puigdomènech Badia, A., Mirza, M., Graves, A., Harley, T., Lillicrap, T.P., Silver, D., Kavukcuoglu, K., 2016. Asynchronous Methods for Deep Reinforcement Learning.
- Moreira-Matias, L., Gama, J., Ferreira, M., Mendes-Moreira, J., Damas, L., 2013. Predicting Taxi-Passenger Demand Using Streaming Data Index Terms-Autoregressive integrated moving average (ARIMA), data streams, ensemble learning, Global Positioning System (GPS) data, mobility intelligence, taxi-passenger demand, time-series forecasting, time-varying Poisson

- models. *IEEE TRANSACTIONS ON INTELLIGENT TRANSPORTATION SYSTEMS* 14, 1393. <https://doi.org/10.1109/TITS.2013.2262376>
- Müller, J., Bogenberger, K., 2015. Time Series Analysis of Booking Data of a Free-Floating Carsharing System in Berlin. *Transportation Research Procedia* 10, 345–354. <https://doi.org/10.1016/J.TRPRO.2015.09.084>
- Narayanan, S., Chaniotakis, E., Antoniou, C., 2020. Shared autonomous vehicle services: A comprehensive review. *Transp Res Part C Emerg Technol* 111, 255–293. <https://doi.org/10.1016/J.TRC.2019.12.008>
- Oda, T., Joe-Wong, C., 2018. MOVI: A Model-Free Approach to Dynamic Fleet Management. *Proceedings - IEEE INFOCOM* 2018-April, 2708–2716. <https://doi.org/10.1109/INFOCOM.2018.8485988>
- Pavone, M., Smith, S.L., Frazzoli, E., Rus, D., 2012. Robotic load balancing for mobility-on-demand systems. *Int J Rob Res* 31, 839–854. <https://doi.org/10.1177/0278364912444766>
- Qin, Z. (Tony), Zhu, H., Ye, J., 2022. Reinforcement learning for ridesharing: An extended survey. *Transp Res Part C Emerg Technol* 144, 103852. <https://doi.org/10.1016/J.TRC.2022.103852>
- Sayarshad, H.R., Chow, J.Y.J., 2017. Non-myopic relocation of idle mobility-on-demand vehicles as a dynamic location-allocation-queueing problem. *Transp Res E Logist Transp Rev* 106, 60–77. <https://doi.org/10.1016/J.TRE.2017.08.003>
- Sayarshad, H.R., Chow, J.Y.J., 2016. Survey and empirical evaluation of nonhomogeneous arrival process models with taxi data. <https://doi.org/10.1002/atr.1401>
- Singh, A., Al-Abbasi, A.O., Member, Student, Aggarwal, V., Member, Senior, 2021. A Distributed Model-Free Algorithm for Multi-Hop Ride-Sharing Using Deep Reinforcement Learning; A Distributed Model-Free Algorithm for Multi-Hop Ride-Sharing Using Deep Reinforcement Learning. <https://doi.org/10.1109/TITS.2021.3083740>
- Sutton, R.S., Barto, A.G., 2015. Reinforcement learning: an introduction, 2nd ed. The MIT Press.
- NYC Taxi & Limousine Commission, 2022. TLC Trip Record Data - TLC [WWW Document]. City of New York. URL <https://www1.nyc.gov/site/tlc/about/tlc-trip-record-data.page> (accessed 7.31.22).
- Tong, Y., Chen, Y., Zhou, Z., Chen, L., Wang, J., Yang, Q., Ye, J., Lv, W., 2017. The Simpler The Better: A Unified Approach to Predicting Original Taxi Demands based on Large-Scale Online Platforms. <https://doi.org/10.1145/3097983.3098018>
- Zhong, C., Batty, M., Manley, E., Wang, J., Wang, Z., Chen, F., Schmitt, G., 2016. Variability in Regularity: Mining Temporal Mobility Patterns in London, Singapore and Beijing Using Smart-Card Data. *PLoS One* 11, 149222. <https://doi.org/10.1371/journal.pone.0149222>